

Design, synthesis and antiproliferative activity evaluation of fluorine-containing chalcone derivatives

Serdar Burmaoglu , Derya Aktas Anil , Arzu Gobek , Deryanur Kilic , Derya Yetkin , Nizami Duran & Oztekin Algul

To cite this article: Serdar Burmaoglu , Derya Aktas Anil , Arzu Gobek , Deryanur Kilic , Derya Yetkin , Nizami Duran & Oztekin Algul (2020): Design, synthesis and antiproliferative activity evaluation of fluorine-containing chalcone derivatives, Journal of Biomolecular Structure and Dynamics, DOI: [10.1080/07391102.2020.1848627](https://doi.org/10.1080/07391102.2020.1848627)

To link to this article: <https://doi.org/10.1080/07391102.2020.1848627>

 View supplementary material [↗](#)

 Published online: 17 Nov 2020.

 Submit your article to this journal [↗](#)

 Article views: 43

 View related articles [↗](#)

 View Crossmark data [↗](#)



Design, synthesis and antiproliferative activity evaluation of fluorine-containing chalcone derivatives

Serdar Burmaoglu^a, Derya Aktas Anil^b, Arzu Gobek^a, Deryanur Kilic^a, Derya Yetkin^c, Nizami Duran^d and Oztekin Algul^e

^aDepartment of Chemistry, Faculty of Science, Atatürk University, Erzurum, Turkey; ^bDepartment of Chemistry and Chemical Process Technologies, Erzurum Vocational High School, Atatürk University, Erzurum, Turkey; ^cAdvanced Technology Education Research and Application Center, Mersin University, Mersin, Turkey; ^dDepartment of Medical Microbiology, Medical Faculty, Mustafa Kemal University, Antakya-Hatay, Turkey; ^eDepartment of Pharmaceutical Chemistry, Faculty of Pharmacy, Mersin University, Mersin, Turkey

Communicated by Ramaswamy H. Sarma

ABSTRACT

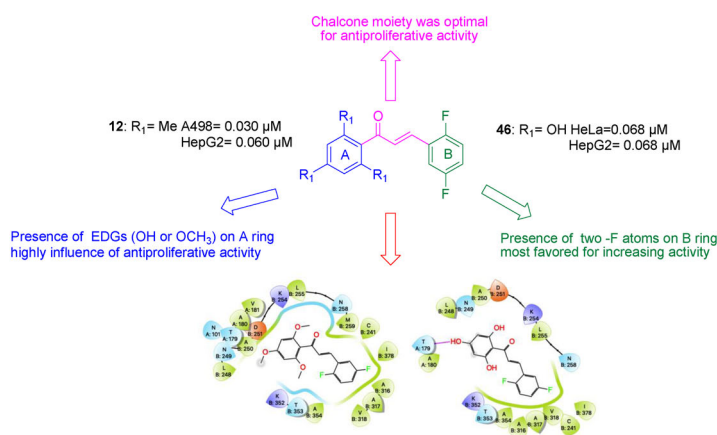
A series of new chalcones containing fluoro atom at B ring have been designed, synthesized, and evaluated to be antiproliferative activity against a panel of human tumor cell lines. Some of the analogs (**8**, **9**, **12**, **45**, **46** and **48**) displayed powerful antiproliferative effects to certain human tumor cells, but all of them were devoid of any cytotoxicity towards the normal HEK 293. Acridine orange staining data supported that the cytotoxic and antiproliferative effects of the synthesized analogs on tumor cells are mediated through apoptosis. The compounds **12** and **46** manifested concentration-dependent antiproliferative activity in human hepatocellular carcinoma cell lines using an xCELLigence assay. The structures and antiproliferative activity relationship were further supported by in silico molecular docking study of the compounds against tubulin protein which suggests our compounds interference to cell division.

ARTICLE HISTORY

Received 13 April 2020
Accepted 4 November 2020

KEYWORDS

Synthesis; Chalcone; MTT; antiproliferative activity; fluor effect



Introduction

Cancer disease is one of the leading causes of death worldwide. Prevalence of various cancer types has nearly doubled within recent years. With this increased rate in mind, if new drugs and therapeutic methods cannot be developed, this rate is expected to increase even further within the coming years (Singh et al., 2014). Although there are currently many treatment methods, the rapidly increasing rates of the disease prevalence urge researchers for developing safer, more

potent and more selective anti-cancer agents. Presence of chalcone-compounds as main components or as a substituent in biologically active molecules encourages medicinal chemists to synthesize chalcone-containing derivatives. Also known as α,β -unsaturated ketones, chalcones are not only good precursors for synthetic derivatization, but also an important component of natural products (Singh et al., 2014). Chalcones and their synthetic analogs have considerable number of biological activities (Karthikeyan et al., 2014). Although in literature, there are many known methods to

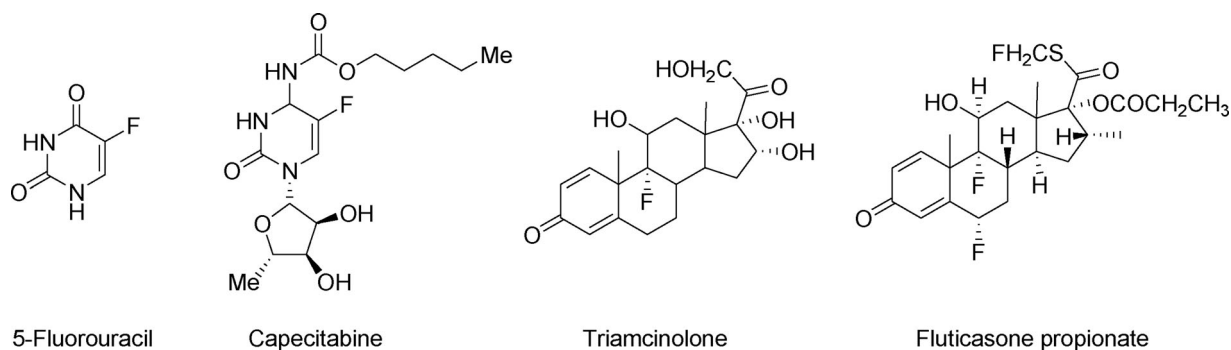


Figure 1. Selected examples of fluorinated drugs.

synthesize chalcones, in general, chalcones can be readily synthesized with a Claisen-Schmidt condensation reaction in the presence of an acid or a base (Matos et al., 2015). Molecules that contain multiple pharmacophores are known to be much more beneficial in treatment of cancer (Abbot et al., 2017).

On the other hand, fluorine is the 13th most common element found on Earth. Despite this fact, it is quite rare in natural organic products, with currently only 13 natural organic products known to include fluorine atom within their structures (Mena et al., 2013). Also, it is becoming increasingly common in the synthetic derivatives, in parallel with the increasing number of medicinal chemistry studies on pharmaceutical compounds including fluorine atom. For instance, the rate of fluorine-containing pharmaceutical compounds was about 2% back in 1970s, whereas now it is around 18%. In USA, 9 out of 31 new drugs that were licensed in 2002 contain fluorine in their structure (Figure 1). Thus, it can be said that the proportion of drugs that contain at least one fluorine atom is 25% in the whole world. When we consider that organofluorine compounds are rare in natural products, this 25% is obviously a quite high rate (Bégué & Bonnet-Delpon, 2008).

Due to its unique properties, fluorine atom is increasingly being incorporated to the structure of small bioactive molecules. However, despite the supportive findings related to the structure-activity relationship, biological effects of fluorine atom are still not exactly clear. Surely, many effects of the fluorine atom indicate that if fluorine is strategically bound to appropriate site of the molecule, it results in very important changes in the biological properties of the molecule compared to the non-fluorine derivatives of the same molecule. Nonetheless, for certain situations, even all this knowledge fails to aid in predicting the effect of fluorine atom on the entire pharmacokinetics. Therefore, determination of its effect still continues as a trial and error process (Isanbor & O'Hagan, 2006). Thus, organofluorine compounds in medicinal chemistry still have significance for the purpose of understanding the enigmatic effect of introduction of fluorine atom to the molecular structure.

Thus, we have recently reported a preliminary account on a new and facile route to chalcones containing fluoro atom at B ring. The results of preliminary *in vitro* antiproliferative activity confirmed that the fluoro-substituted chalcones at B ring inhibited the growth of certain human cancer cell lines

(Burmaoglu et al., 2016). In particular, it has been determined that the molecules whose literature data are designed will have high efficiency in five cancer cells.

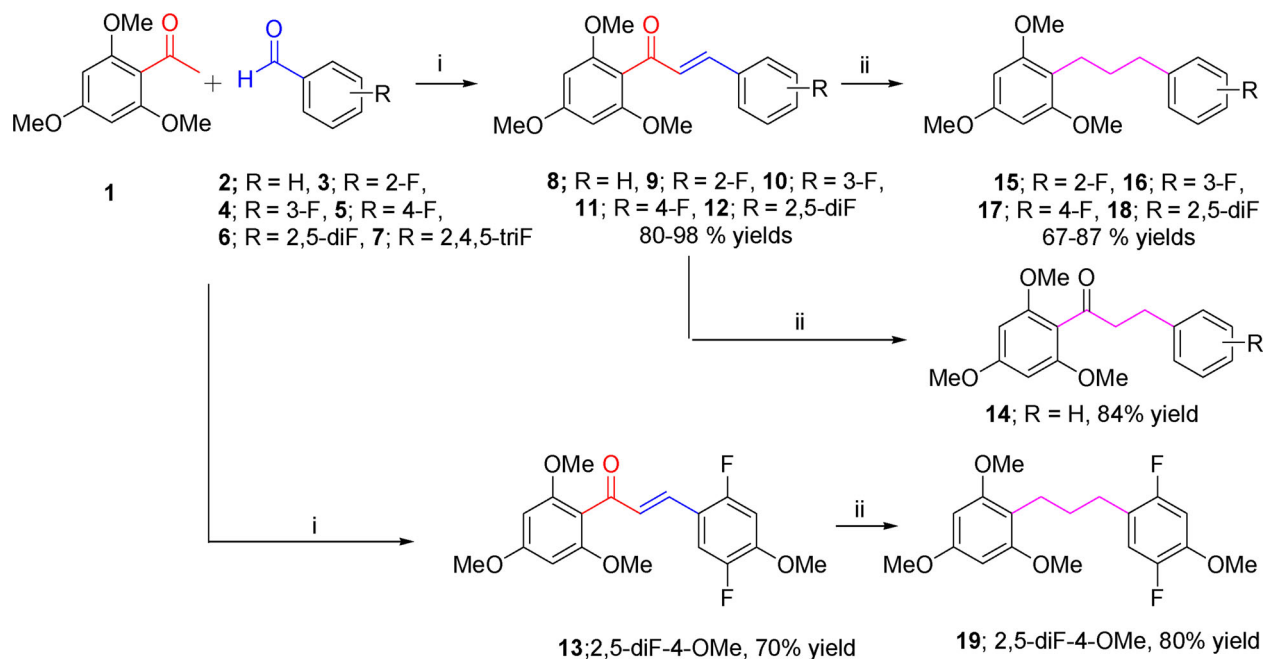
Based upon these observations, we designed and synthesized a series of chalcone derivatives containing fluorine atom at different positions of a series of B-ring and their antiproliferative properties against various cancer cell lines were investigated.

Finally, the antiproliferative activities of thirty-four new synthesized chalcone and dihydrochalcone derivatives (**11**, **13**, **17**, **19**, **22-33**, **42**, **44**, **45**, **48**, **50**, **51**, **61-66**, **68-73**) were evaluated. In addition, the previously synthesized twelve chalcones/dihydrochalcones (**8-10**, **12**, **14-16**, **18**, **43**, **46**, **49** and **52**) were included only for comparison purposes. The primary objective of the synthesis of the fluoro-substituted chalcone derivatives was to determine their potency and specificity against five different cancer cells compared with those of methotrexate (MTX). Acridine orange staining and MTT (3-(4,5-dimethylthiazol-2-yl)-2,5-diphenyl tetrazolium bromide) assay were conducted on different cancer cell types in the presence of our derivatives in order to measure their apoptotic as well as antiproliferative activities, respectively. The concentration-dependent antiproliferative activities of the highest active compounds against HepG2 cell line were also revealed using an xCELLigence assay. The structure activity properties were further supported by *in silico* molecular docking study of their interaction with the tubulin protein.

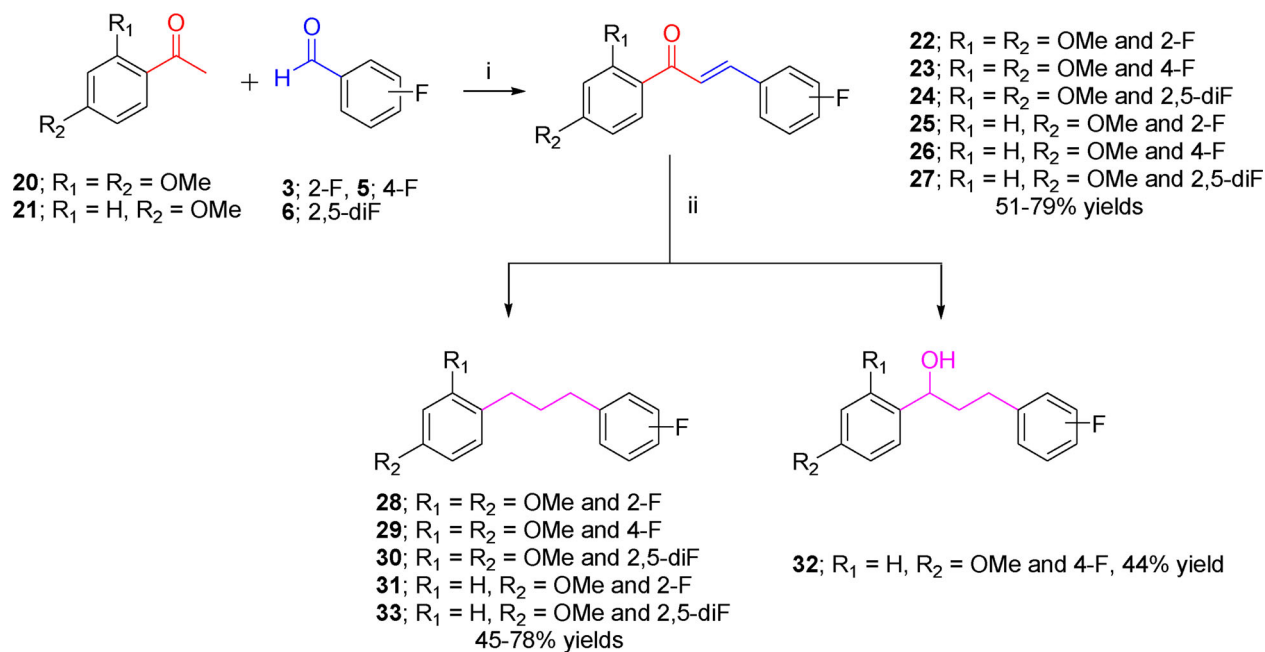
Results and discussion

Chemistry

As shown in Scheme 1, the target compounds **8-13** and **14-19** were synthesized. The condensation of trimethoxyacetophenone (**1**) with benzaldehyde (**2**) and fluoro-substituted benzaldehydes (**3-7**) in an aqueous solution of KOH afforded related chalcones **8-13** in 70-92% yields through the adoption of a general synthesis protocol (Burmaoglu et al., 2016). In this series, the reaction between 2,4,5-trifluoro benzaldehyde (**7**) and trimethoxy acetophenone (**1**) resulted in compound **13**. The fluorine atom at para position of compound **7** is very suitable for nucleophilic aromatic substitution. Since this reaction is carried out in methanol and in strong basic condition, the methoxide ion readily reacts with the fluorine atom at the para position to give compound **13**. Hydrogenation of trimethoxychalcones **8-13** on Pd/C



Scheme 1. Preparation of fluoro-substituted trimethoxy chalcones (**8-13**) and dihydrochalcones (**14-19**). Reagents and conditions: (i) KOH, MeOH, room temperature, 15 h; (ii) H₂, Pd-C, EtOH, room temperature, 16 h.

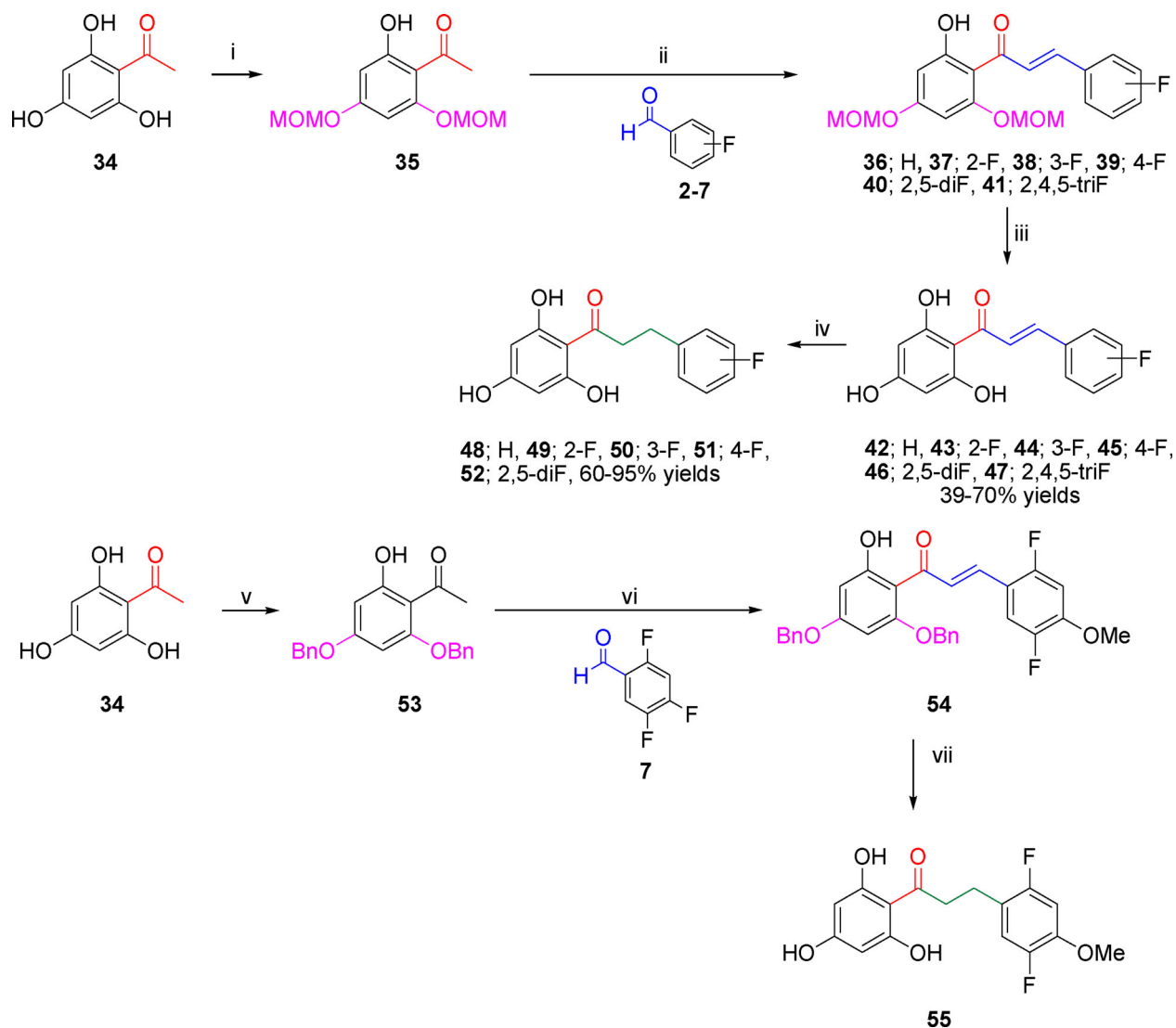


Scheme 2. Preparation of fluoro-substituted mono/di-methoxychalcones (**22-27**) and dihydrochalcones (**28-33**). Reagents and conditions: (i) KOH, MeOH, room temperature, 15 h; (ii) H₂, Pd-C, EtOH, room temperature, 16 h.

afforded related dihydrochalcones **14-19** in 67-87% yields (Scheme 1).

To synthesize fluoro-substituted mono/di-methoxy chalcones and their dihydrochalcone derivatives (**22-27** and **28-33**) we used the same method above. For this, the condensation of di or mono-methoxyacetophenone (**20** or **21**) with fluoro-substituted benzaldehydes (**3**, **5**, and **6**) in an aqueous solution of KOH afforded related chalcones **22-27** in 51-79% yields. Hydrogenation of mono/di-methoxychalcones **22-27** on Pd/C afforded related dihydrochalcones **28-33** in 44-78% yields (Scheme 2).

Condensation of trihydroxyacetophenone (**34**) with benzaldehyde (**2**) and fluoro-substituted benzaldehydes (**3-7**) did not afford the related chalcones and only the starting materials were recovered. Because of this setback, we decided to use a protective group for the hydroxyl groups. For this, chloromethyl methyl ether (MOMCl), which is stable under basic conditions and can be deprotected easily under mild acidic conditions, was used. After the base-catalysed reaction of compound **35** with related benzaldehydes **2-7**, the related chalcones, except compound **47**, were gotten by removal of MOM with HCl in MeOH. As a result of the reaction between



Scheme 3. Preparation of fluoro-substituted tri-hydroxychalcones (**42-47**) and dihydrochalcones (**48-52** and **55**). Reagents and conditions: (i) MOMCl, DIPEA, DCM, 0 °C, 3 h; (ii) KOH, MeOH, room temperature, 15 h; (iii) HCl, room temperature, 12 h; (iv) H₂, Pd-C, EtOH, room temperature, 16 h; (v) BnBr, K₂CO₃, DMF, room temperature, 12 h, under N₂; (vi) KOH, MeOH, room temperature, 15 h; (vii) H₂, Pd-C, EtOH, room temperature, 16 h.

compound **35** and **7** a mixture of product was obtained and could not be separated in any way by chromatographic methods for compound **47**. Therefore, we decided to use benzyl chloride instead of MOMCl as a protecting group. Condensation of **53** with compound **7** pleasingly afforded related benzyl-protected chalcone **54**. Hydrogenation of tri-hydroxychalcones **42-46** on Pd-C afforded related dihydrochalcones **48-52** in 64-95% yields. Hydrogenation of **54** on Pd-C did not afford the related dihydrochalcone **55**. We got a mixture of products and this mixture could not be separated in any way by chromatographic methods for compound **55** (Scheme 3).

To synthesize fluoro-substituted dihydroxy chalcones, we used the same synthetic route of the trihydroxy chalcones. For this, the reaction between **56** and fluoro-substituted benzaldehydes (**3-6**) did not afford the related chalcones and only the starting materials were recovered. Then we used MOM-protected acetophenone **57** instead of compound **56** and condensation of **57** with fluoro-substituted benzaldehydes **3-6** gave related MOM-protected chalcones **58-60**. After the removal of MOM with HCl in MeOH gave related

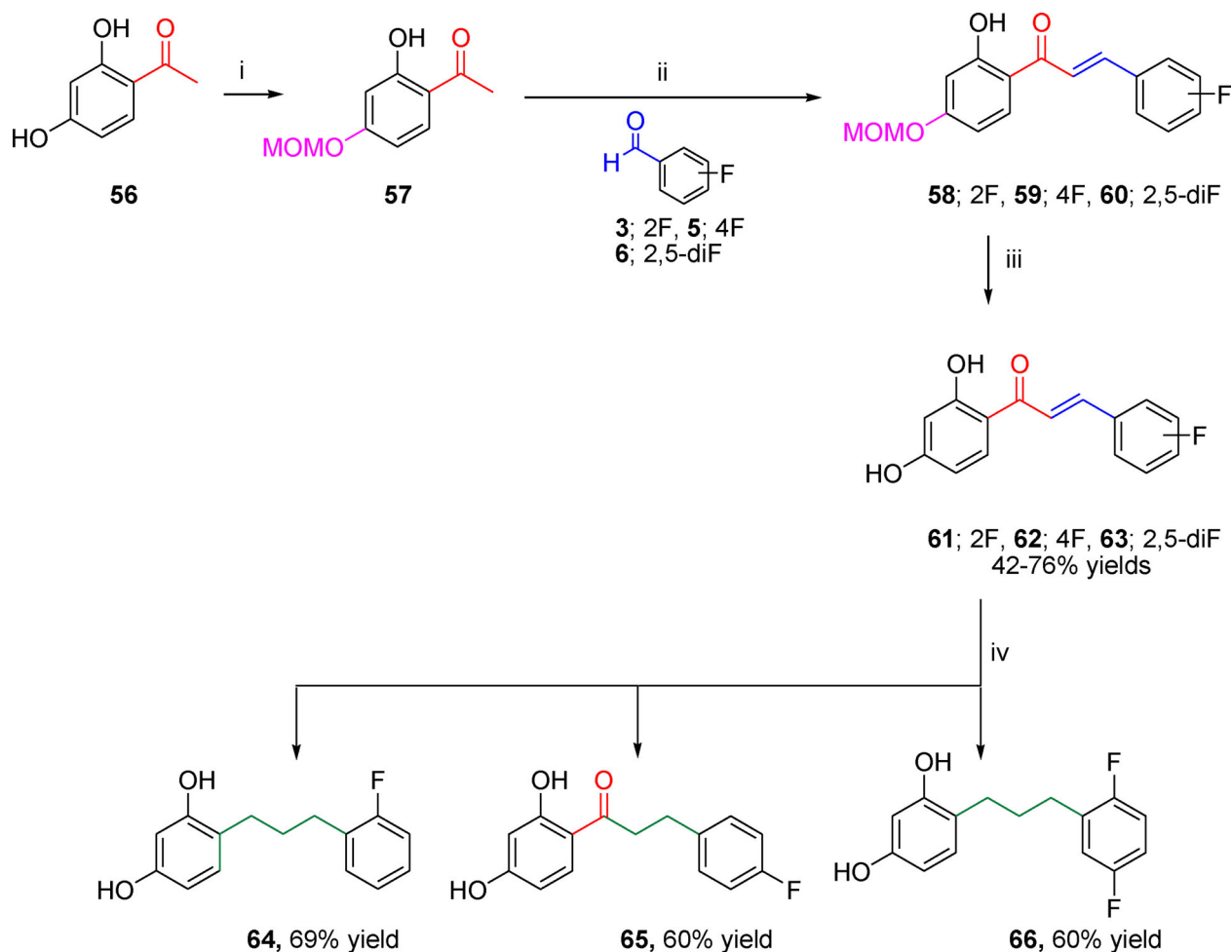
chalcones **61-63** in 42-76% yields. Hydrogenation of compounds **61-63** in the presence of Pd-C gave related dihydrochalcones **64-66** in 60-69% yields (Scheme 4).

Finally, preparation of fluoro-substituted monohydroxy chalcones was summarized in Scheme 5. For this, we did not need to protect the hydroxyl group with any protecting group. Condensation of **67** with related benzaldehydes **3-6** gave related chalcones **68-70** in 54-83% yields and hydrogenation of **68-70** in the presence of Pd-C gave desired products **71-73** in 50-54% yields.

Consequently, five class of chalcone and dihydrochalcone derivatives were synthesized according to functional group differences in ring A as shown in Figures 2 and 3.

Biological evaluation

After successful completion of the synthesis studies, all synthesized compounds were evaluated for their *in vitro* antiproliferative activities against a panel of five human malignant cell lines, including human lung adenocarcinoma epithelial



Scheme 4. Preparation of fluoro-substituted dihydrochalcones (**61-63**) and dihydrochalcones (**64-66**). Reagents and conditions: (i) MOMCl, DIPEA, DCM, 0 °C, 3 h; (ii) KOH, MeOH, room temperature, 15 h; (iii) HCl, room temperature, 12 h; (iv) H₂, Pd-C, EtOH, room temperature, 16 h.

cell line (A549), human renal cancer cell line (A498), human cervical cancer cell line (HeLa), human skin malignant melanoma cell line (A375), human hepatocellular cell line (HepG2) and normal cell lines; human embryonic kidney cell line (HEK 293) and compared with those of methotrexate (MTX).

Then, in order to further strengthen our MTT data, we calculated the apoptotic indexes of chalcone derivatives at 8 and 24 h time points by acridine orange staining test (Figure 4a-e). Compounds with the highest activities were further examined by using acridine orange dye that stains the cytoplasmic changes during the apoptosis as well as by using ethidium bromide that would indicate the chromosomal changes through its binding to DNA. The samples were analyzed by immuno-fluorescence microscope. Our compounds effects were compared to that of the methotrexate, MTX. Apoptotic indexes were determined by measuring the levels of cell and nucleus shrinkage, chromatin condensation, and accumulation of the nuclear envelope at the periphery. Both the floating and adherent cells were analyzed after 8th and 24th hours of incubation, 100 cells were counted in the same square area to calculate the apoptotic index of each sample.

Cell growth inhibition was evaluated by using the standard MTT colorimetric assay after exposure of cells to the test compounds for 96 h. The commercial antitumor agent MTX was used as positive control (Table 1).

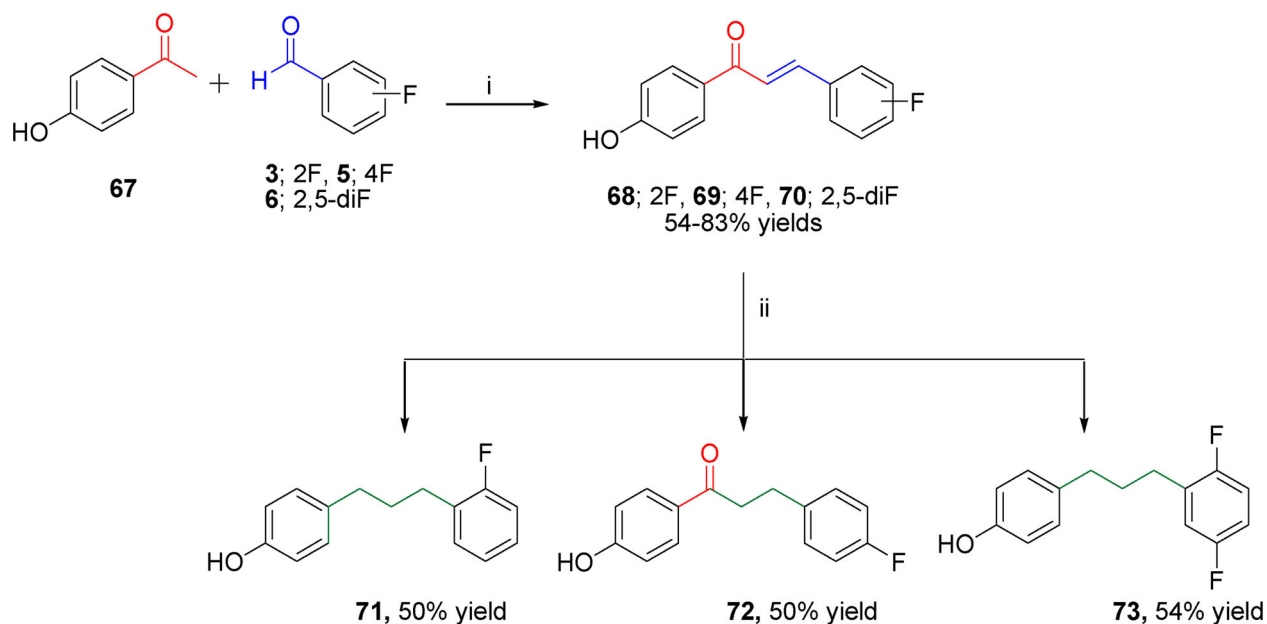
Inhibitory studies in vitro antiproliferative activities and structure-activity relationship (SAR)

To assess the specificity of the compounds, their toxicity was tested against normal cells using HEK. The specificity of the compounds was calculated as their IC₅₀ values for normal cells divided by their IC₅₀ values for the specific cancer cells, according to the specificity equation (Specificity = IC₅₀ values of compound against normal cells/IC₅₀ values of compound against cell line of interest). The specificity of the compounds appeared to be relatively moderate specificity toward all cancer cells.

The non-toxic concentrations of all compounds were determined on the HEK-293 cell line. Then, antiproliferative activity studies were performed at these non-toxic concentrations. The compounds with the best selectivity values for each cancer cell line are shown in Table 2.

The synthesized compounds were mono/di/tri methoxy or hydroxy substituted analogs of chalcone with varying components: fluorine atoms, ketone groups, or alkyl chains. Accordingly, a structure-activity relationship (SAR) was established by comparing the antiproliferative activities of the different chalcone groups.

According to the resulting IC₅₀ values of the cytotoxic assay, potency and specificity (Table 1) the A549, A498, HeLa, A375, and HepG2 cell lines were medium and sensitive to all of the synthesized analogues. The highest potency in the



Scheme 5. Preparation of fluoro-substituted mono-hydroxychalcones (**68-70**) and dihydrochalcones (**71-73**). Reagents and conditions: (i) KOH, MeOH, room temperature, 15 h; (ii) H₂, Pd-C, EtOH, room temperature, 16 h.

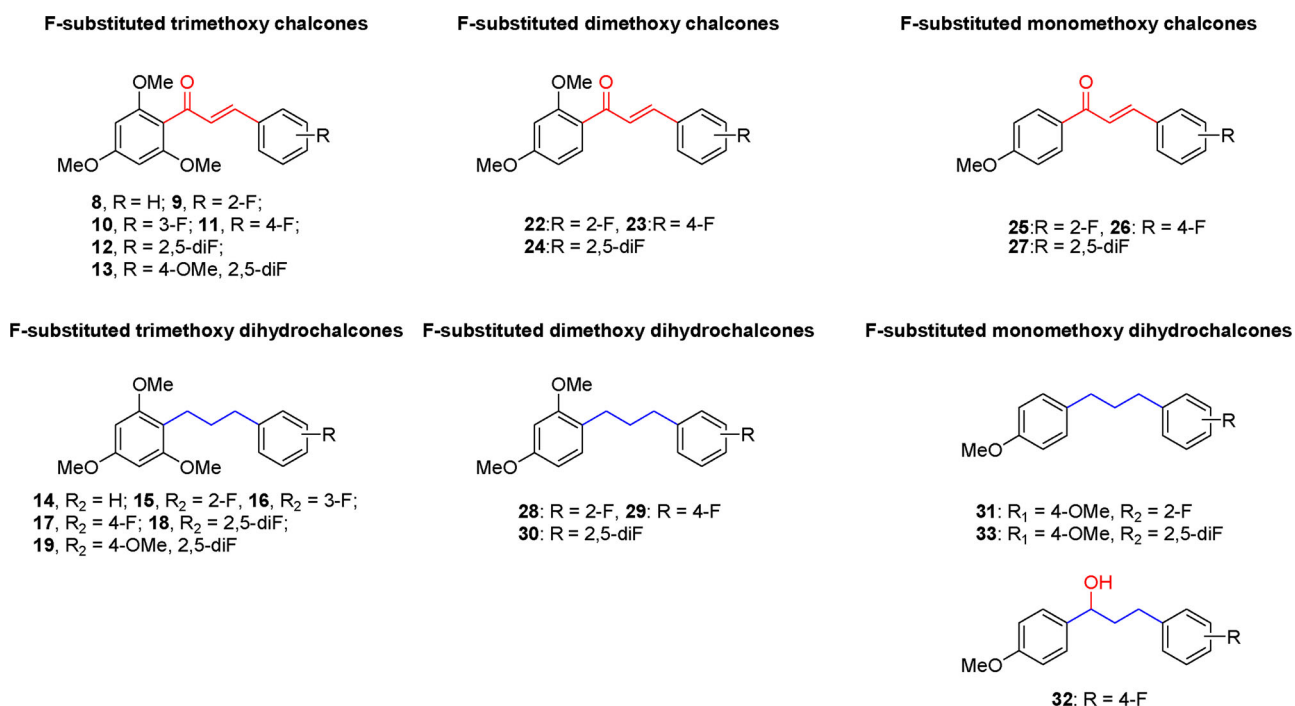


Figure 2. The structures of fluoro-substituted methoxy chalcones/dihydrochalcones.

culture of A549, A498 was recorded after treatment with trihydroxy/trimethoxy in A ring and non/2-F/and 2,5-diF substituted in B ring on chalcone derivatives **46** and **8**, **9** and **12** (IC₅₀: 0.067 – 0.137 μM), which demonstrated about approximately 6-fold lower potency than the antitumor agents MTX. A potent submicromolar antiproliferative activity was recorded after treatment of A549 cells with trihydroxy and difluoro substituted saturated chalcone derivative **52** (IC₅₀: 0.136 μM), and dihydroxy and 2,5-difluoro substituted saturated chalcone derivative **66** (IC₅₀: 0.150 μM) and monohydroxy and 4-fluoro substituted chalcone derivative **69** (IC₅₀: 0.160 μM).

The highest active molecules against A498 cell lines were the following compounds: trimethoxy (A ring) and nonsubstituted or 2,5-diF (B ring) chalcone derivatives **8** (IC₅₀: 0.067 μM), and **12** (IC₅₀: 0.030 μM), and trihydroxy (A ring) and nonsubstituted (B ring) saturated chalcone derivative **48** (IC₅₀: 0.15 μM), respectively, which exhibited 4 and 1.8 or 9-fold lower potency than MTX.

Several compounds exhibited submicromolar activities toward the HeLa cells. These are **12** and **16** (IC₅₀: 0.060 and 0.066 μM), trimethoxy (A ring) and 2,5-difluoro (B ring) chalcone and trimethoxy (A ring) 3-F (B ring) saturated chalcone, respectively. Also, trihydroxy (A ring) and 2,5-difluoro (B ring)

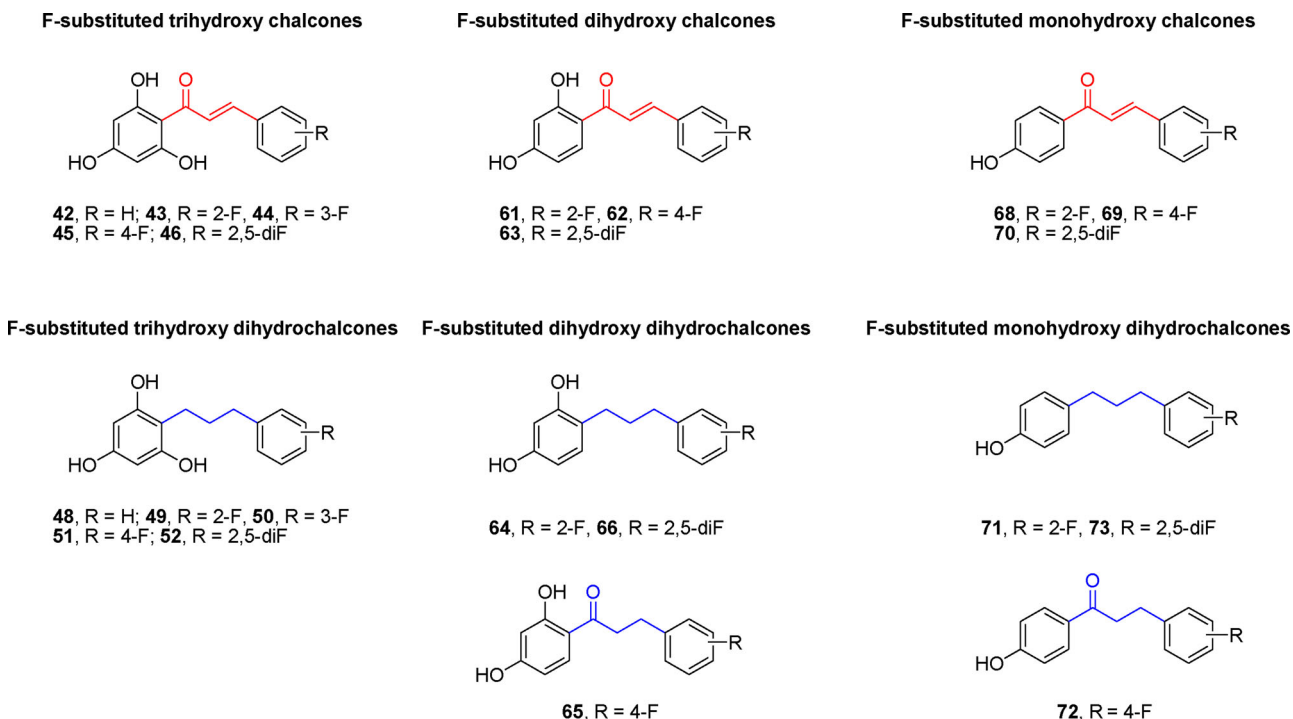


Figure 3. The structures of hydroxy chalcones/dihydrochalcones.

unsaturated and saturated chalcone derivatives **46**, and **52** (IC_{50} : $0.068 \mu M$) had significantly active against cancer cell line, respectively.

The most potent compound in the culture of A375 cell was analogue trihydroxy (A ring) 2,5-difluoro (B ring) chalcone **52** (IC_{50} : $0.068 \mu M$), which demonstrated about 3.5-fold lower potency than MTX, in contrast to mono/di methoxy and mono/di hydroxy chalcone and saturated chalcone derivatives, which was completely inactive against this cell line. But, trimethoxy (A ring) and nonsubstituted or 2,5-diF (B ring) unsaturated chalcone derivatives (**8** and **12**) were the most active compounds against to A375 cancer cell lines, 0.067 and $0.060 \mu M$, respectively.

The highest potency in the HepG2 cell line was recorded after treatment with **12** (IC_{50} : $0.060 \mu M$), trimethoxy (A ring) 2,5-diF (B ring); **43** (IC_{50} : $0.029 \mu M$) trihydroxy (A ring) 2-F (B ring), and **46** (IC_{50} : $0.068 \mu M$) trihydroxy (A ring) 2,5-diF (B ring) which exhibited approximately 1 and 2-fold lower potency than MTX.

In order to correlate the structure of synthesized chalcone derivatives with their cytotoxic activities, we first considered the effect of fluorine atoms at B ring. None substituted compounds; **8**, **14**, **42** and **48** have been used as controls in this SAR analysis. As the data in Table 1 reveal the introduction of fluorine atom caused the increased antitumor potency originally displayed by control compounds, especially 2,5-diF compounds. As the data in Table 1 indicate the removal of fluorine atom decreased antiproliferative activity, against majority of tumor cell lines under evaluation.

The next round of modifications undertaken to improve the antiproliferative activities have been performed by chalcone structure to saturated chalcone structure of linker group of two phenyl rings. The relationships between these structural changes and antiproliferative potencies were

established by comparing the IC_{50} values of analogues with those recorded for the corresponding linker group should be saturated.

Remarkably, all of the synthesized chalcones and saturated chalcones including mono and dimethoxy, mono and dihydroxy completely inactive toward all cell lines, in contrast to trihydroxy and trimethoxy group of compounds and MTX, which exhibited a potency cytotoxic activities (IC_{50} : 0.03 - $9.91 \mu M$ and $0.022 \mu M$ respectively) against this cell lines. These results do suggest that the synthesized chalcones represent selective antitumor agents, but this assumption should be verified by additional *in vitro* experiments with additional normal cell lines.

Based on the initial survey that we showed in Table 2, indicating the selectivity of the compounds with non-toxic concentrations of each compound on each cancer cell type. In our further investigations, we focused on the compounds with the highest selectivity at the lowest concentration on each cell line.

The selected compounds and MTX were exposed for a period of 0–96 h for each cancer cell line. At the end of the incubation, all cells were evaluated and subjected to an assessment of their cytotoxic responses using an MTT assay (Figures 5–9) (McGahon et al., 1995; Mosmann, 1983).

As shown in 5-9, the proliferation of cancer cells treated with a non-toxic and in lower concentration dose of compounds and MTX was inhibited in a time-dependent manner. After a short treatment (24 h), MTX was more effective and the amount of live cells was lower than that observed with the compounds. The antiproliferative activity of all the tested compounds increased as the exposure time was extended, as proven by the decline in the number of surviving cells. After a longer exposure, all tested compounds had an activity equal to that of MTX.

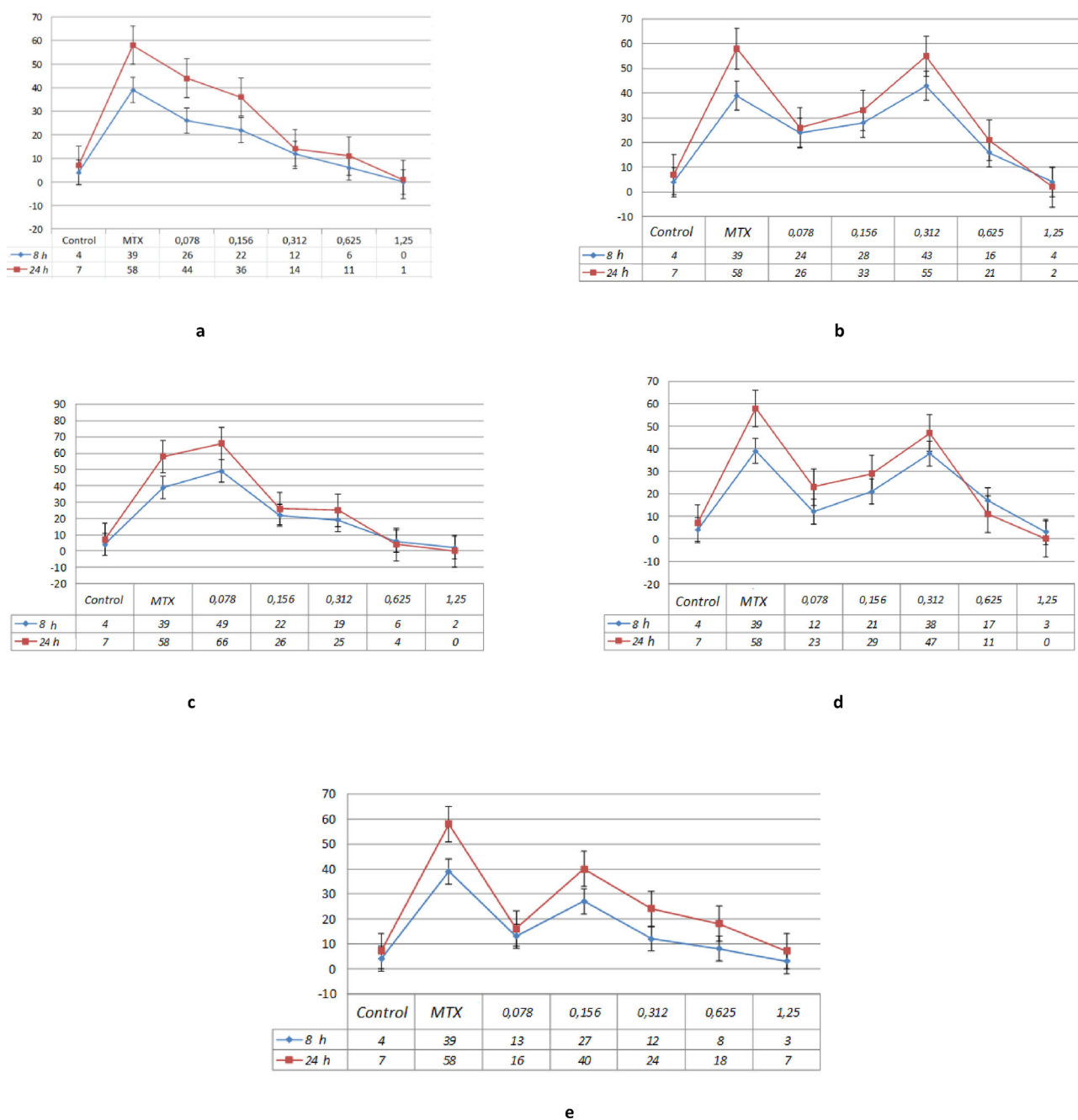


Figure 4. a. Apoptotic cell index of compound “12” in A549 cell culture; b. Apoptotic cell index of compound “48” in A489 cell culture; c. Apoptotic cell index of compound “12” in HeLa cell culture; d. Apoptotic cell index of compound “12” in A375 cell culture; e. Apoptotic cell index of compound “12” in HepG2 cell culture.

Detection of apoptosis by acridine orange staining test

In order to further strengthen our MTT data, we did acridine orange staining on the cancer cell lines treated with the chalcone derivatives with the highest specificity as well as activity against them. After their careful evaluation at 8 and 24 h time points, we calculated their apoptotic indexes as shown in Figure 4a-e. In line with MTT assay data appropriate compounds exerted anticancer effect on each cancer cell line in a dose and time dependent manner by inducing the apoptosis. These results hint the possible intracellular pathway of antiproliferative effect of our compounds on each cancer cell type. Apoptosis was the main route of their anticancer activities based on acridine orange staining. Our compounds and MTX

control reagent had comparable effects on the cancer cells. Overall, this data supports high efficiency of the newly generated chalcone derivatives on versatile cancer cell types. Their activities and specificities against the cancer cell types ranged based on the differences in their structures.

xCELLigence cytotoxicity protocol

The use of the xCELLigence system for label-free and real-time monitoring of cell viability was described here. The monitoring of cell viability by the xCELLigence system was made it possible to distinguish between different perturbations of cell viability. We have used the cell index

Table 1. *In vitro* cytotoxicity of fluoro-substituted chalcones analogues and MTX.

| Comp. No | Structure Substituent Trimethoxy | HEK293 | A549 | A498 | Hela | A375 | HepG2 | Specificity* | | | | |
|-------------|----------------------------------|------------------------------------|-------|-------|-------|-------|-------|--------------|-------|-------|-------|-------|
| | | IC ₅₀ (μM) ^a | | | | | | | A549 | A498 | Hela | A375 |
| 8 | – | 0.335 | 0.134 | 0.067 | 0.134 | 0.067 | 0.134 | 2.5 | 5.0 | 2.5 | 5.0 | 2.5 |
| 9 | 2-F | 0.632 | 0.126 | 0.126 | 0.126 | 0.126 | 0.126 | 5.0 | 5.0 | 5.0 | 5.0 | 5.0 |
| 10 | 3-F | 0.632 | 0.253 | 0.126 | 0.506 | 0.506 | 0.253 | 2.5 | 5.0 | 1.25 | 1.25 | 2.5 |
| 11 | 4-F | 3.161 | 0.253 | 0.253 | 4.047 | 1.265 | 1.265 | 12.5 | 12.5 | 0.8 | 2.5 | 2.5 |
| 12 | 2,5-diF | 0.598 | 0.120 | 0.030 | 0.060 | 0.060 | 0.060 | 5.0 | 20.0 | 10.0 | 10.0 | 10.0 |
| 13 | 2,5-DiF-4-OMe | 9.91 | 4.95 | 9.91 | 2.48 | 1.24 | 9.91 | 2.00 | 1.00 | 4.00 | 7.99 | 1.00 |
| 14 | – | 1.665 | 0.533 | 0.533 | 0.533 | 0.533 | 0.533 | 3.125 | 3.1 | 3.125 | 3.125 | 3.125 |
| 15 | 2-F | 1.643 | 0.526 | 0.526 | 0.263 | 0.526 | 0.263 | 3.125 | 3.1 | 6.25 | 3.125 | 6.25 |
| 16 | 3-F | 0.657 | 0.263 | 0.526 | 0.066 | 0.263 | 0.263 | 2.5 | 1.3 | 10.0 | 2.5 | 2.5 |
| 17 | 4-F | 8.21 | 1.03 | 1.03 | 1.03 | 2.05 | 2.05 | 7.97 | 7.97 | 1.00 | 0.50 | 0.50 |
| 18 | 2,5-diF | 1.551 | 0.248 | 0.248 | 0.248 | 0.496 | 0.496 | 6.3 | 6.3 | 6.25 | 3.125 | 3.125 |
| 19 | 2,5-DiF-4-OMe | 7.35 | 1.84 | 7.35 | 1.84 | 1.84 | 3.67 | 3.99 | 1.00 | 3.99 | 3.99 | 2.00 |
| Dimethoxy | | | | | | | | | | | | |
| 22 | 2-F | 1.09 | 0.27 | 0.27 | 0.54 | 0.27 | 0.54 | 4.04 | 4.04 | 2.02 | 4.04 | 2.02 |
| 23 | 4-F | 2.18 | 2.18 | 2.18 | 1.09 | 1.09 | 1.09 | 1.00 | 1.00 | 2.00 | 2.00 | 2.00 |
| 24 | 2,5-diF | 4.11 | 1.03 | 1.03 | 1.03 | 1.03 | 1.03 | 3.99 | 3.99 | 3.99 | 3.99 | 3.99 |
| 28 | 2-F | 1.22 | 9.76 | 2.44 | 4.88 | 9.76 | 4.88 | 0.13 | 0.50 | 0.25 | 0.13 | 0.25 |
| 29 | 4-F | 4.88 | 4.88 | 9.76 | 4.88 | 2.44 | 2.44 | 1.00 | 0.50 | 1.00 | 2.00 | 2.00 |
| 30 | 2,5-diF | 2.28 | 2.28 | 4.56 | 9.12 | 2.28 | 1.14 | 1.00 | 0.50 | 0.25 | 1.00 | 2.00 |
| Monomethoxy | | | | | | | | | | | | |
| 25 | 2-F | 2.28 | 0.28 | 0.57 | 0.57 | 0.57 | 0.28 | 8.14 | 4.00 | 4.00 | 4.00 | 8.14 |
| 26 | 4-F | 2.28 | 1.14 | 1.14 | 2.28 | 2.28 | 1.14 | 2.00 | 2.00 | 1.00 | 1.00 | 2.00 |
| 27 | 2,5-diF | 2.14 | 0.53 | 0.53 | 0.53 | 1.07 | 0.53 | 4.04 | 4.04 | 4.04 | 2.00 | 4.04 |
| 31 | 2-F | 2.56 | 1.28 | 1.28 | 0.64 | 1.28 | 1.28 | 2.00 | 2.00 | 4.00 | 2.00 | 2.00 |
| 32 | 4-F | 0.64 | 0.32 | 0.64 | 0.32 | 1.28 | 0.16 | 2.00 | 1.00 | 2.00 | 0.50 | 4.00 |
| 33 | 2,5-diF | 1.19 | 0.59 | 0.30 | 0.30 | 0.59 | 0.59 | 2.02 | 3.97 | 3.97 | 2.02 | 2.02 |
| Trihydroxy | | | | | | | | | | | | |
| 42 | – | 2.44 | 0.61 | 0.61 | 0.61 | 0.61 | 0.61 | 4.00 | 4.00 | 4.00 | 4.00 | 4.00 |
| 43 | 2-F | 0.365 | 0.146 | 0.729 | 2.334 | 0.146 | 0.029 | 2.5 | 0.5 | 0.156 | 2.5 | 12.5 |
| 44 | 3-F | 4.56 | 1.14 | 1.14 | 2.28 | 1.14 | 1.14 | 4.00 | 4.00 | 2.00 | 4.00 | 4.00 |
| 45 | 4-F | 2.28 | 0.57 | 0.57 | 0.28 | 0.14 | 0.14 | 4.00 | 4.00 | 8.14 | 16.29 | 16.29 |
| 46 | 2,5-diF | 1.711 | 0.137 | 0.274 | 0.068 | 0.274 | 0.068 | 12.5 | 6.3 | 25.0 | 6.25 | 25.0 |
| 48 | – | 2.42 | 0.15 | 0.15 | 0.30 | 0.30 | 0.30 | 16.13 | 16.13 | 8.07 | 8.07 | 8.07 |
| 49 | 2-F | 1.810 | 0.145 | 0.145 | 0.579 | 0.579 | 0.290 | 12.5 | 12.5 | 3.125 | 3.125 | 6.25 |
| 50 | 3-F | 1.19 | 0.15 | 0.30 | 0.30 | 0.59 | 0.59 | 7.93 | 3.97 | 3.97 | 2.02 | 2.02 |
| 51 | 4-F | 1.19 | 0.30 | 0.15 | 1.19 | 1.19 | 0.30 | 3.97 | 7.93 | 1.00 | 1.00 | 3.97 |
| 52 | 2,5-diF | 0.340 | 0.136 | 0.136 | 0.068 | 0.068 | 0.136 | 2.5 | 2.5 | 5.0 | 5.0 | 2.5 |
| Dihydroxy | | | | | | | | | | | | |
| 61 | 2-F | 1.20 | 0.30 | 0.30 | 0.60 | 0.30 | 0.30 | 4.00 | 4.00 | 2.00 | 4.00 | 4.00 |
| 62 | 4-F | 1.21 | 0.30 | 0.30 | 0.15 | 0.60 | 0.60 | 4.03 | 4.03 | 8.07 | 2.02 | 2.02 |
| 63 | 2,5-diF | 0.56 | 1.13 | 1.13 | 1.13 | 2.26 | 2.26 | 0.50 | 0.50 | 0.50 | 0.25 | 0.25 |
| 64 | 2-F | 2.54 | 5.08 | 2.54 | 5.08 | 5.08 | 2.54 | 0.50 | 1.00 | 0.50 | 0.50 | 1.00 |
| 65 | 4-F | 2.40 | 0.30 | 0.30 | 0.60 | 1.20 | 0.60 | 8.00 | 8.00 | 4.00 | 2.00 | 4.00 |
| 66 | 2,5-diF | 1.18 | 0.15 | 0.15 | 0.59 | 1.18 | 0.15 | 7.87 | 7.87 | 2.00 | 1.00 | 7.87 |
| Monohydroxy | | | | | | | | | | | | |
| 68 | 2-F | 2.58 | 0.32 | 0.32 | 0.64 | 1.29 | 0.32 | 8.06 | 8.06 | 4.03 | 2.00 | 8.06 |
| 69 | 4-F | 1.29 | 0.16 | 0.64 | 0.64 | 0.64 | 0.32 | 8.06 | 2.02 | 2.02 | 2.02 | 4.03 |
| 70 | 2,5-diF | 2.40 | 1.20 | 1.20 | 1.20 | 1.20 | 1.20 | 2.00 | 2.00 | 2.00 | 2.00 | 2.00 |
| 71 | 2-F | 2.71 | 0.34 | 0.17 | 0.34 | 2.71 | 0.34 | 7.97 | 15.94 | 7.97 | 1.00 | 7.97 |
| 72 | 4-F | 2.60 | 0.65 | 1.30 | 0.16 | 1.30 | 1.30 | 4.00 | 2.00 | 16.25 | 2.00 | 2.00 |
| 73 | 2,5-diF | 5.12 | 0.32 | 0.64 | 0.32 | 0.64 | 0.32 | 16.00 | 8.00 | 16.00 | 8.00 | 16.00 |
| | MTX | 0.028 | 0.025 | 0.016 | 0.022 | 0.020 | 0.041 | 1.12 | 1.75 | 1.27 | 1.40 | 0.68 |

^aIC₅₀ is the concentration of compound required to inhibit the cell growth by 50% compared to an untreated control. Values are means of three independent experiments. Coefficients of variation were less than 10%. HEK293, human embryonic kidney cells; A549, human lung adenocarcinoma epithelial cells; A498, human renal cancer cells; HeLa, human cervical cancer cells; A375, human skin malignant melanoma cells; HepG2, Human hepatocellular carcinoma cell lines. *Specificity of the compounds: the ratio for each compound of its IC₅₀ value for normal cells (HEK293) to its IC₅₀ value for the cancer cell.

Table 2. The compounds with the best selectivity values and non-toxic concentrations for each cancer cell line (human nontoxic concentration).

| Cancer cell line | The highest selective compound | Non-toxic concentration (μM) |
|------------------|--------------------------------|------------------------------|
| A549 | 12 and 48 | 0.12 and 0.15 |
| A498 | 12 and 48 | 0.03 and 0.15 |
| HeLa | 12 and 46 | 0.06 and 0.068 |
| A375 | 12 and 45 | 0.06 and 0.14 |
| HepG2 | 12 and 46 | 0.029 and 0.068 |

determination on monitoring of viability by xCELLigence to systematically examine cytotoxic effects triggered with different cell-killing kinetics. Good correlation was observed and

the significance of time resolution by xCELLigence readout was exemplified by its ability to pinpoint the optimal time points for conducting end point viability and apoptosis assays. The specificity of the compounds **12** and **46** determined to be cell-dependent with good specificity toward HepG2 cells. Therefore, these compounds were selected for xCELLigence assay. In order to evaluate the cytotoxicity response of BJ-5ta homo sapiens foreskin normal cell line and the liver cancer cells to the compound **12** and **46** applications, the time-dependent graph of the proliferation curves obtained from the real-time cell analyzer was plotted.

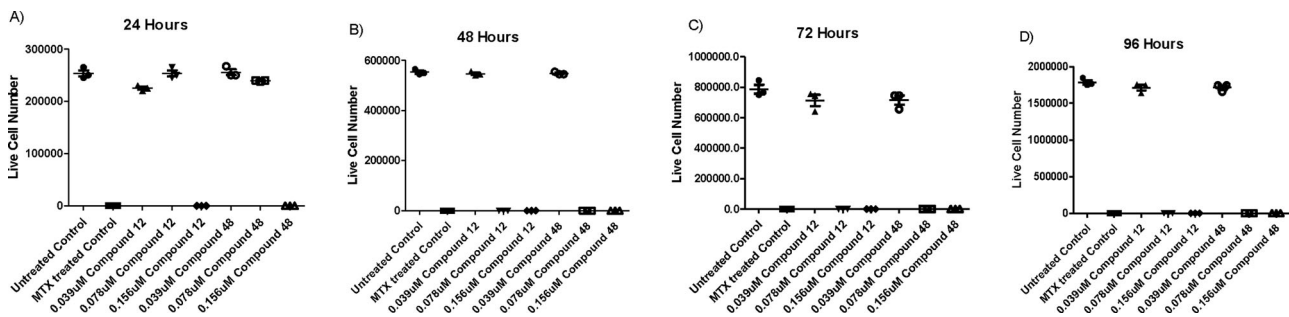


Figure 5. MTT assay on Human Lung Adenocarcinoma Epithelial Cells (A549 cell line) after 24, 48, 72 and 96 h incubation periods with methotrexate and compounds. The absorbance values were measured at 570 nm for the MTT assay. Control cells were untreated and MTX treated cells were used as positive controls. Cell viability was calculated based on the ratio of the absorbance of the sample groups over those of the untreated group. P values were calculated by student t test by using at least three independent experimental values.

Note: p values: Concentration: 0.039 = Control-12: $p > .05$; Control-48: $p > .05$; Concentration: 0.078 = Control-12: $p < .001$; Control-48: $p < .001$; Concentration: 0.156 = Control-12: $p < .0001$; Control-48: $p < .0001$; Control-MTX: $p < 0.001$

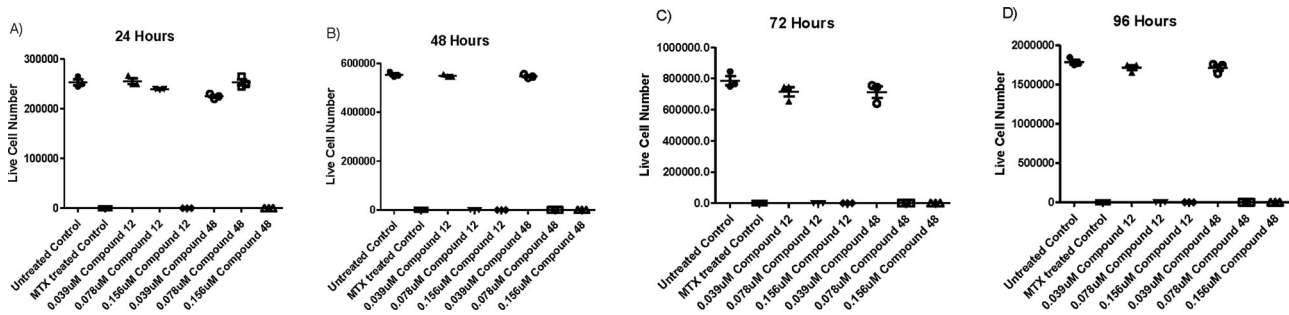


Figure 6. MTT assay on A498 Cell (Human Renal Cancer Cells) after 24, 48, 72 and 96 h incubation periods with methotrexate and compounds. The absorbance values were measured at 570 nm for the MTT assay. Control cells were untreated and MTX treated cells were used as positive controls. Cell viability was calculated based on the ratio of the absorbance of the sample groups over those of the untreated group. P values were calculated by student t test by using at least three independent experimental values.

Note: p values: Concentration: 0.039 = Control-12: $p > .05$; Control-48: $p > .05$; Concentration: 0.078 = Control-12: $p < .001$; Control-48: $p < .001$; Concentration: 0.156 = Control-12: $p < .001$; Control-48: $p < .001$; Control-MTX: $p < 0.001$

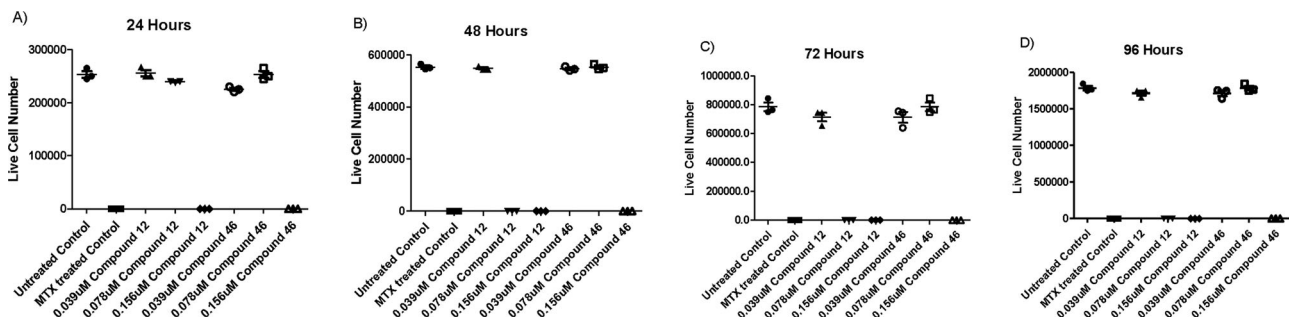


Figure 7. MTT assay on HeLa after 24, 48, 72 and 96 h incubation periods with methotrexate and compounds. The absorbance values were measured at 570 nm for the MTT assay. Control cells were untreated and MTX treated cells were used as positive controls. Cell viability was calculated based on the ratio of the absorbance of the sample groups over those of the untreated group. P values were calculated by student t test by using at least three independent experimental values.

Note: p values: Concentration: 0.039 = Control-12: $p > .05$; Control-46: $p > .05$; Concentration: 0.078 = Control-12: $p < .001$; Control-46: $p > .05$; Concentration: 0.156 = Control-12: $p < .001$; Control-46: $p < .001$; Control-MTX: $p < 0.01$

Compounds 12 and 46 effects the proliferation of BJ-5ta cells. BJ-5ta homo sapiens foreskin normal cell line was used to evaluate the effect of compounds **12** and **46** on normal cells. The cell proliferation of all concentrations (39 nM, 78 nM, and 158 nM) and 24, 48 and 72 h after the application of **12** (Figures 10, 11 and 12) and **46** (Figures 13, 14 and 15) (Table 3) compounds in BJ-5ta (ATCC® CRL-4001™) cell line was compared to the control group.

As shown in Figures 10, 11, and 12, a correlation is not significantly observed between the concentration of compound **12** and cytotoxic response kinetics, cell index and cell viability. It was determined that compound **46** such as

compound **12**, it is not significant differences between the same correlation (Figures 13, 14, and 15). The statistical accuracy of the data is shown in Table 3. The decrease in cell proliferation of all concentrations 24, 48 and 72 h after the application of **12** and **46** compounds in BJ-5ta cell line was not significant compared to the control group ($p = 0,059$). As a result, the values indicate that all **12** and **46** concentrations had a no significant antiproliferative effect on BJ-5ta cell line.

Compound 12 and 46 effects the proliferation of HepG2 cells. In order to evaluate the cytotoxicity response of the

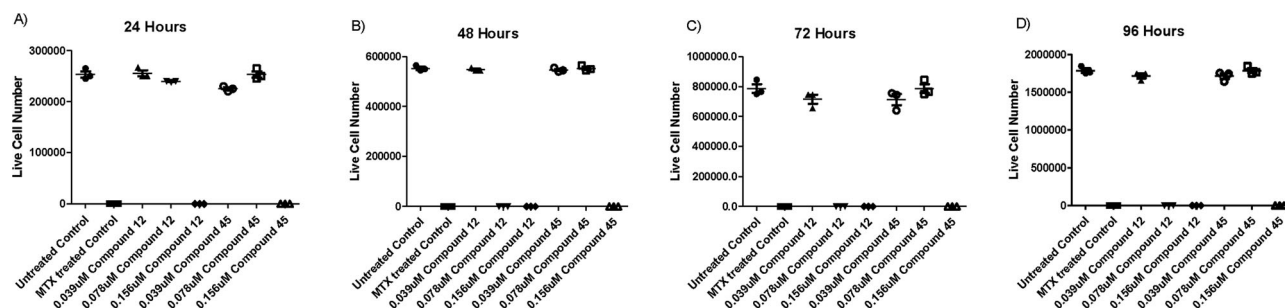


Figure 8. MTT assay on A375 Cell (Human Skin Malignant Melanoma Cells) after 24, 48, 72 and 96 h incubation periods with methotrexate and compounds. The absorbance values were measured at 570 nm for the MTT assay. Control cells were untreated and MTX treated cells were used as positive controls. Cell viability was calculated based on the ratio of the absorbance of the sample groups over those of the untreated group. P values were calculated by student t test by using at least three independent experimental values.

Note: p values: Concentration: 0.039 = Control-12: $p > .05$; Control-45: $p < .001$; Concentration: 0.078 = Control-12: $p < .001$; Control-45: $p < .001$; Concentration: 0.156 = Control-12: $p < .001$; Control-45: $p < .001$; Control-MTX: $p < 0.01$

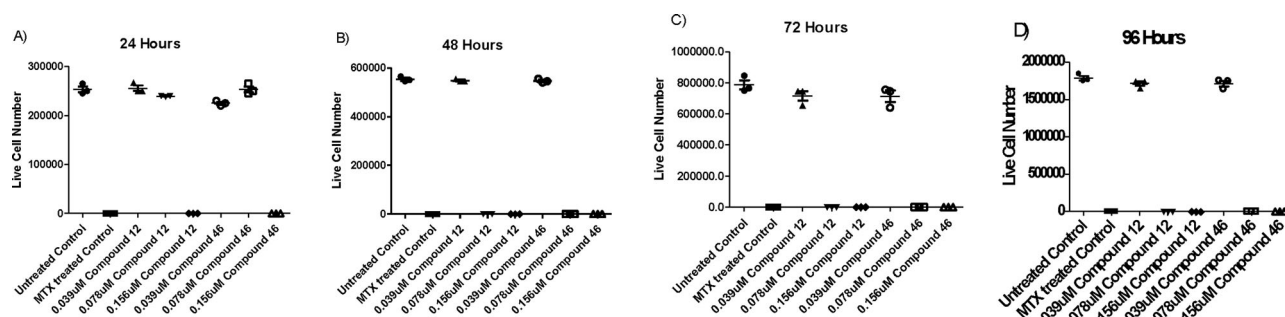


Figure 9. MTT assay on HepG2 Cell (Human Hepatocellular Carcinoma Cells) after 24, 48, 72 and 96 h incubation periods with methotrexate and compounds. The absorbance values were measured at 570 nm for the MTT assay. Control cells were untreated and MTX treated cells were used as positive controls. Cell viability was calculated based on the ratio of the absorbance of the sample groups over those of the untreated group. P values were calculated by student t test by using at least three independent experimental values.

Note: p values: Concentration: 0.039 = Control-12: $p > .05$; Control-46: $p > .05$; Concentration: 0.078 = Control-12: $p < .001$; Control-46: $p > .05$; Concentration: 0.156 = Control-12: $p < .001$; Control-46: $p < .001$; Control-MTX: $p < 0.01$

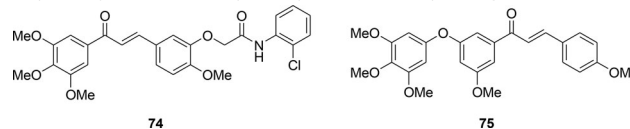
liver cancer cells to the **12** and **46** substance applications, the time-dependent graph of the proliferation curves obtained from the real-time cell analyser was plotted. The data obtained were digitized in terms of cell index by the software of the device (Figures 16–20).

As a result of the experiment (Figures 16–20), the difference between the mean values of the control group and the other group before administration of the substance ($p > 0.05$), the difference between the mean measurements taken at 24, 48 and 72 h after the **12** and **46** applications was statistically significant ($p < 0.001$). After 12 administration 24 h (39 nM ($p < 0.001$), 78 nM ($p = 0.001$) and 158 nM ($p = 0.031$)) and 48 h (39 nM ($p = 0.002$), 78 nM ($p = 0.011$), 158 nM ($p = 0.021$)) decrease in cell proliferation such as **46** was significant compared to the control group, but there was no significant difference between the groups at 72 h ($p = 0.084$).

Molecular docking studies

Microtubules composed of α and β -tubulin heterodimers are one of the most important structural components of the cell skeleton in eukaryotic cells. These microtubules are involved in many important cellular functions such as cytoplasmic organelle motility, formation of mitotic spindles, and protection of the integrity of the cell shape, intracellular transport and cell replication. A large number of anticancer ligands interfere with the microtubule polymerization/depolymerisation process resulting in the arrest of the cell cycle in the G2/M phase (Choudhury et al., 2013; Qiu

et al., 2017). Many of the clinically used natural product anticancer agents such as colchicines, MDL-27048, taxanes, combretastatin A-4, podophyllotoxin and vinca alkaloids are tubulin-binding agents. Colchicine, combretastatin A-4 and podophyllotoxin are targets for the colchicine domain, while vinblastine targets the vinca alkaloid site, which are known as microtubule destabilizing agents. On the other hand, agents such as paclitaxel that bind to the paclitaxel site are called microtubule-stabilizing agents (Banu et al., 2017). Huang and co-workers have synthesized novel chalcone derivatives (**74**, **75**) and compound **74** has inhibited tubulin polymerization by *in vitro* tubulin polymerization experiments. It has also been shown by molecular docking study that **74** can be binding to the colchicine site of tubulin (Huang et al., 2017). Anti-tubulin polymerization activities and anticancer activities of chalcone derivatives containing the diaryl ether moiety were evaluated by Wang *et al.* In addition thanks to the molecular docking studies, the binding mechanism of **75** in the colchicine binding site of tubulin has been demonstrated (Wang et al., 2020). Based on large number of such literatures results, it has been reported that chalcone derivatives have been as tubulin inhibitors (Kamal et al., 2010; Mirzaei et al., 2020; Sabina et al., 2017).



Thus, in our current study, molecular docking was performed by inserting the compounds into the colchicine

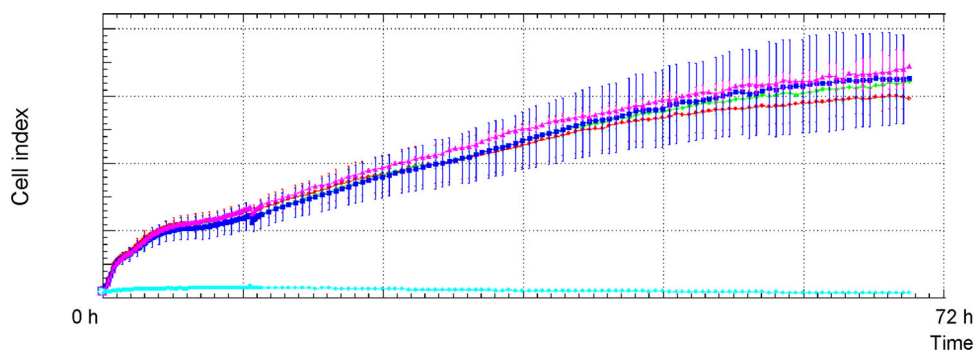


Figure 10. BJ-5ta cell line was treated with various cytotoxic compounds and monitored in real time for cytotoxic response kinetics. Representative compounds **12** generated distinct response profiles. Pink: Control, red: 39 nM, green: 78 nM, navy blue: 158 nM, turquoise: blank.

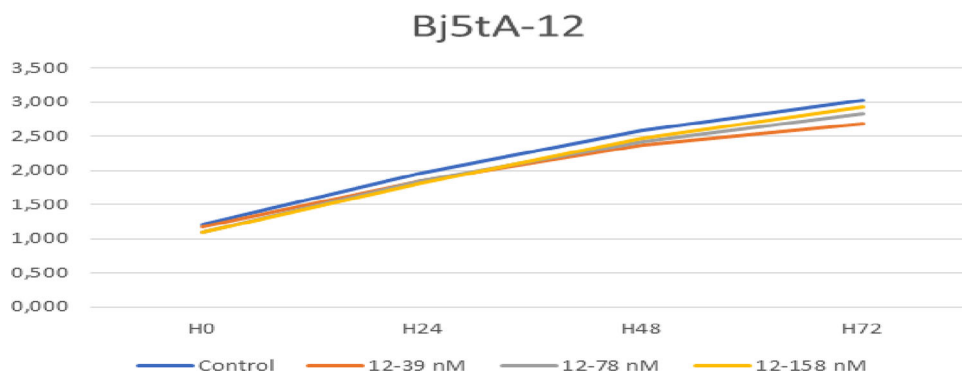


Figure 11. Cell index values of BJ-5ta cells treated with 39, 78, 158 nM of **12**.

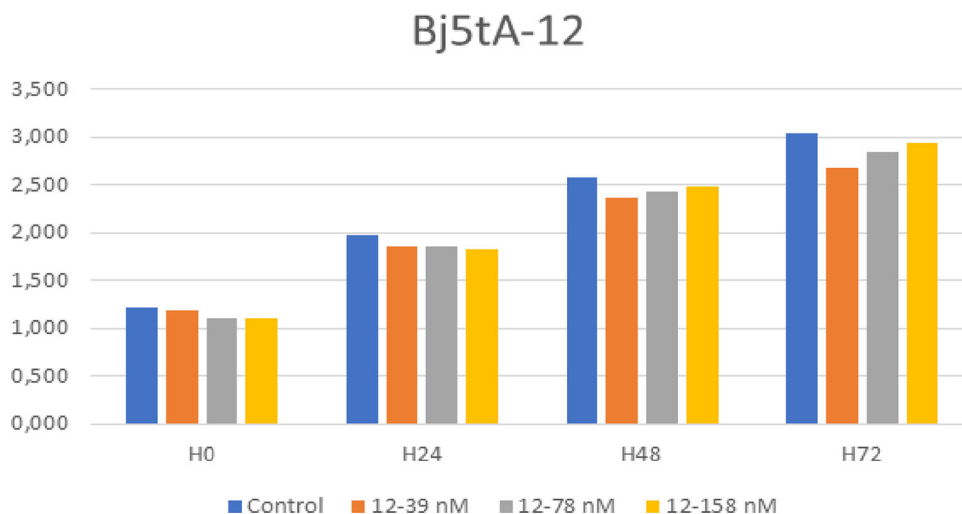


Figure 12. Determination of the concentration of **12** that is required for cell proliferation and cell viability. BJ-5ta cells were incubated with 39, 78 and 158 nM were followed for 72 h using xCELLigence cell analysis system. UT column corresponds to untreated cells and 39, 78, 158 nM concentrations. This allows to follow in real time proliferation of the cells and to image the cells at different times. Representative images after 72 h of treatment are shown for each condition.

binding site of tubulin in order to recognize possible binding mode and key active site interactions. Combretastatin is a natural phenol that has antimetabolic activity that specifically binds to the colchicine binding domain of tubulin (Banu et al., 2017). For this reason, combretastatin was used as a reference molecule in the docking study. The compounds and the reference molecule were docked with tubulin protein to identify possible binding mode and key active site residues.

When the docking results of combretastatin, **12**, **45**, **46** and **48** molecules were examined, it was determined that

the combretastatin formed a hydrogen bond interaction with the Gly A:144 residue and pi-cation interaction with Lys B:254. The compound **45** formed a hydrogen bond with the Asn B:249, the compound **46** formed a hydrogen bond with the Thr A:179. Lastly the compound **48** formed a hydrogen bond with the Val B:238.

The residues Asn B:258, Thr A:179, Ser A:178, Thr B:353, Asn A:101, Thr A:145, Gln B: 247 and Gln A:11 made polar interactions with combretastatin, while the residues Ala A:180, Val A:181, Ala B:354, Ala A:99, Ala A:12 and Leu B:248 made hydrophobic interactions. Also, in the combretastatin

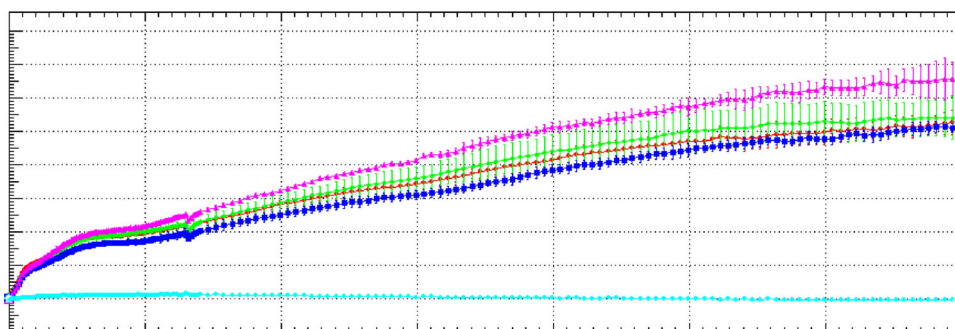


Figure 13. BJ-5ta cell line was treated with various cytotoxic compounds and monitored in real time for cytotoxic response kinetics. Representative compounds **46** generated distinct response profiles. Pink: Control, red: 39 nM, green: 78 nM, navy blue: 158 nM, turquoise: blank.

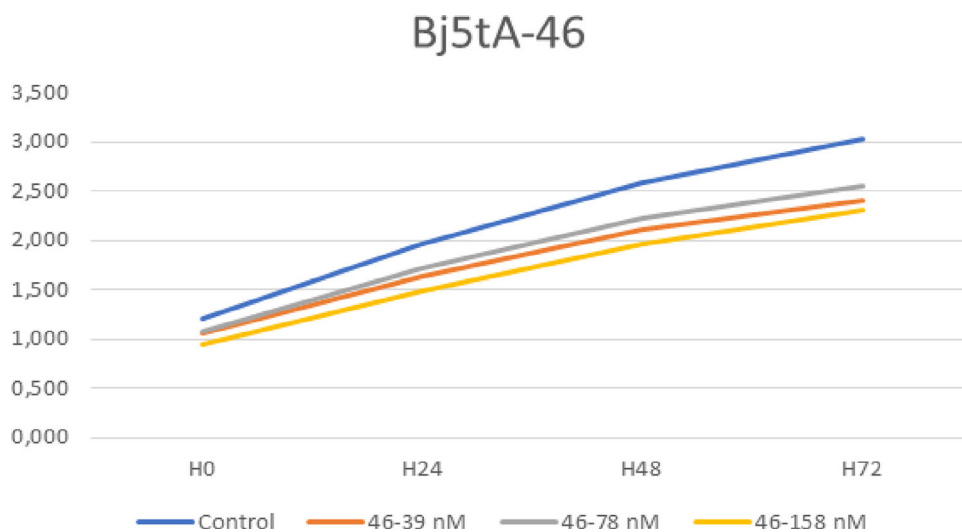


Figure 14. Cell index values of BJ-5ta cells treated with 39,78,158 nM of **46**.

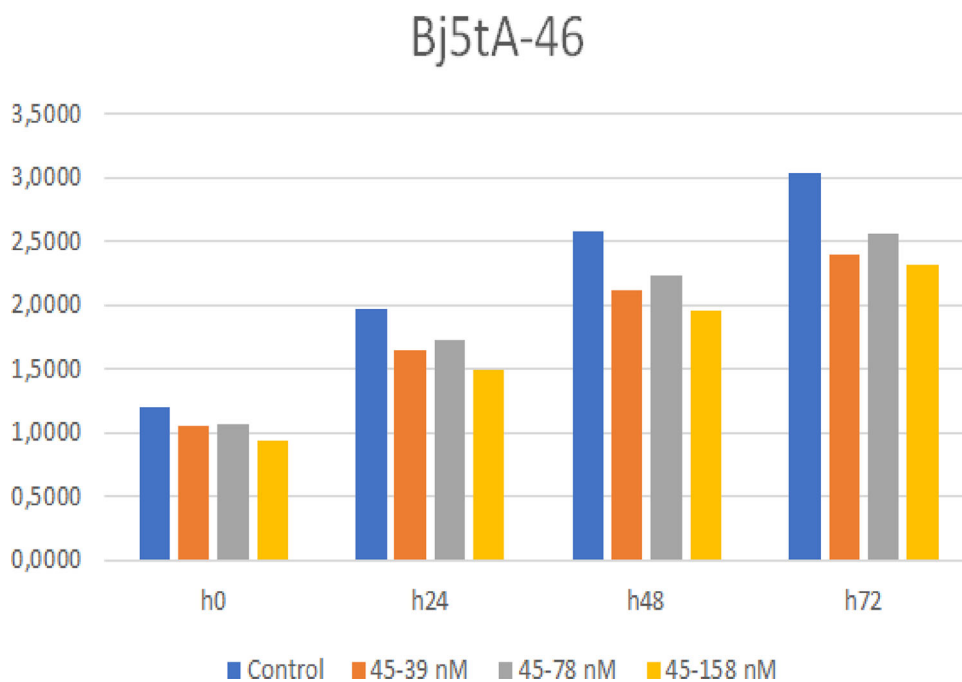
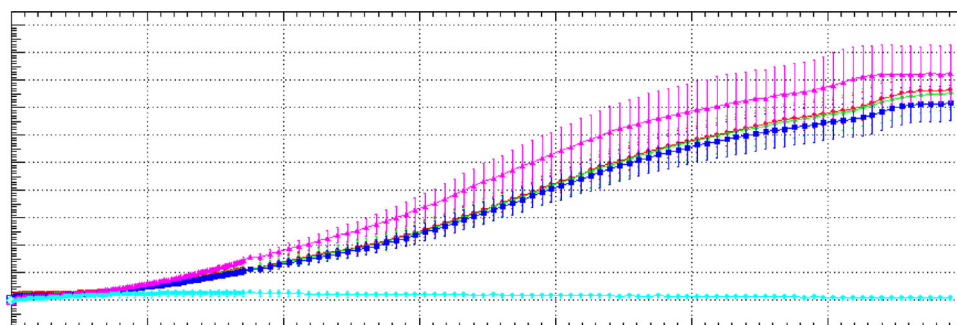
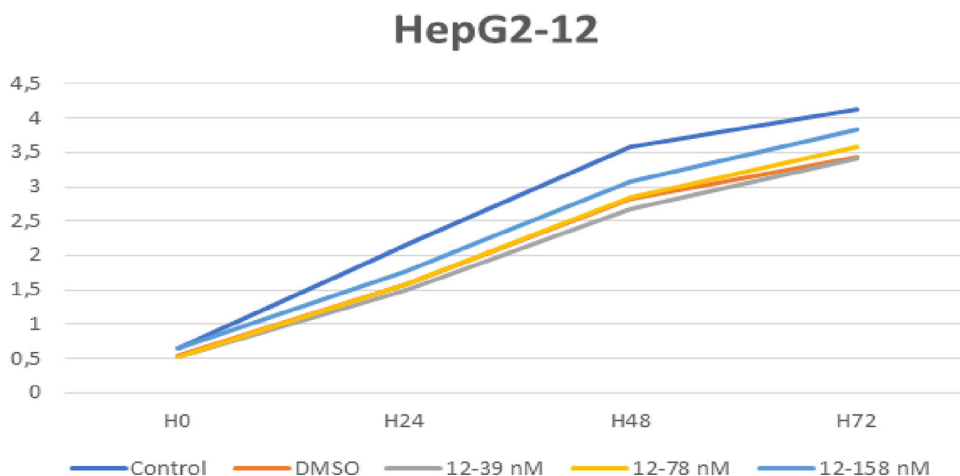


Figure 15. Determination of the concentration of **46** that is required for cell proliferation and cell viability. (A) BJ-5ta cells were incubated with 39, 78 and 158 nM were followed for 72 h using xCELLigence cell analysis system. UT column corresponds to untreated cells and 39,78,158 nM concentrations. This allows to follow in real time proliferation of the cells and to image the cells at different times. Representative images after 72 h of treatment are shown for each condition.

Table 3. Average of measurements between groups 24, 48 and 72 h after 12 and 46 administration.

| | H0 | | H24 | | H48 | | H72 | |
|-----------|-------------------|-------------|-------------------|-------------|-------------------|-------------|-------------------|-------------|
| | Mean \pm SD | Min-Max |
| Control | 1.21 \pm 0.019 | 1.191-1.229 | 1.97 \pm 0.023 | 1.951-1.995 | 2.584 \pm 0.042 | 2.541-2.626 | 3.035 \pm 0.066 | 2.969-3.101 |
| 12-39 nM | 1.179 \pm 0.145 | 1.087-1.396 | 1.856 \pm 0.301 | 1.648-2.302 | 2.373 \pm 0.333 | 2.077-2.849 | 2.682 \pm 0.265 | 2.421-3.04 |
| 12-78 nM | 1.096 \pm 0.063 | 1.044-1.175 | 1.851 \pm 0.057 | 1.781-1.907 | 2.427 \pm 0.112 | 2.272-2.535 | 2.835 \pm 0.182 | 2.61-3.006 |
| 12-158 nM | 1.096 \pm 0.207 | 0.809-1.261 | 1.82 \pm 0.333 | 1.419-2.232 | 2.474 \pm 0.496 | 1.951-3.145 | 2.936 \pm 0.639 | 2.402-3.863 |
| 46-39 nM | 1.059 \pm 0.04 | 1.015-1.107 | 1.638 \pm 0.092 | 1.501-1.702 | 2.117 \pm 0.151 | 1.908-2.269 | 2.405 \pm 0.196 | 2.139-2.598 |
| 46-78 nM | 1.075 \pm 0.082 | 0.984-1.151 | 1.72 \pm 0.169 | 1.574-1.879 | 2.232 \pm 0.272 | 2.013-2.581 | 2.562 \pm 0.312 | 2.298-3.009 |
| 46-158 nM | 0.946 \pm 0.073 | 0.848-1.015 | 1.496 \pm 0.068 | 1.406-1.556 | 1.962 \pm 0.075 | 1.856-2.032 | 2.315 \pm 0.078 | 2.212-2.402 |
| P | | | | | 0,059 | | | |

**Figure 16.** HepG2 cell line was treated with various cytotoxic compounds and monitored in real time for cytototoxic response kinetics. Representative compound 46 generated distinct response profiles. Pink: Control, red: 39 nM, green: 78 nM, navy blue: 158 nM, turquois: blank.**Figure 17.** Cell index values of HepG2 cells treated with 39,78,158 nM of 12.

binding site, positive and negative charge interactions were found with Lys B:352- Lys B:254 and Glu A:71- Asp A:69 residues, respectively. The docking score of combretastatin was determined as $-4.82 \text{ kcal/mol}^{-1}$.

The residues Asn B:258, Thr A:179, Thr B:353, Asn A:101 and Asn B:249 made polar interactions with compound **12**, while the residues Ala A:180, Val A:181, Ala B:354, Leu B:255, Ala B:250, Met B:259, Cys B:241, Ile B:378, Ala B:316, Ala B:317, Val B:318 and Leu B:248 made hydrophobic interactions. Also, in the binding site, positive and negative charge interactions were found with Lys B:352- Lys B:254 and Asp B:251 residues, respectively. The docking score of the compound **12** was determined as $-5.78 \text{ kcal/mol}^{-1}$.

The residues Asn B:258, Thr A:179, Thr B:314, Asn A:101, Gln A:11 and Asn B:249 made polar interactions with compound **45**, while the residues Ala A:180, Val A:181, Leu B:255, Ala B:316, Leu B:248, Ala B:250, Val B:315 and Met B:259 made hydrophobic interactions. Also, in the binding site,

positive and negative charge interactions were found with Lys B:352- Lys B:254 and Asp B:251 residues, respectively. The docking score of the compound **45** was determined as $-7.26 \text{ kcal/mol}^{-1}$.

The residues Asn B:258, Thr A:179, Thr B:353 and Asn B:249 made polar interactions with compound **46**, while the residues Ala A:180, Ala B:354, Leu B:255, Ala B:250, Cys B:241, Ile B:378, Ala B:316, Ala B:317, Val B:318 and Leu B:248 made hydrophobic interactions. Also, in the binding site, positive and negative charge interactions were found with Lys B:352- Lys B:254 and Asp B:251 residues, respectively. The docking score of the compound **46** was determined as $-6.04 \text{ kcal/mol}^{-1}$.

The residues Asn B:258, Thr A:179 and Thr B:239 made polar interactions with compound **48**, while the residues Ala A:180, Val A:181, Met B:259, Leu B:255, Ala B:354, Ala B:250, Cys B:241, Ile B:378, Ala B:316, Ala B:317, Val B:318, Val B:238, Leu B:242 and Leu B:248 made hydrophobic interactions.

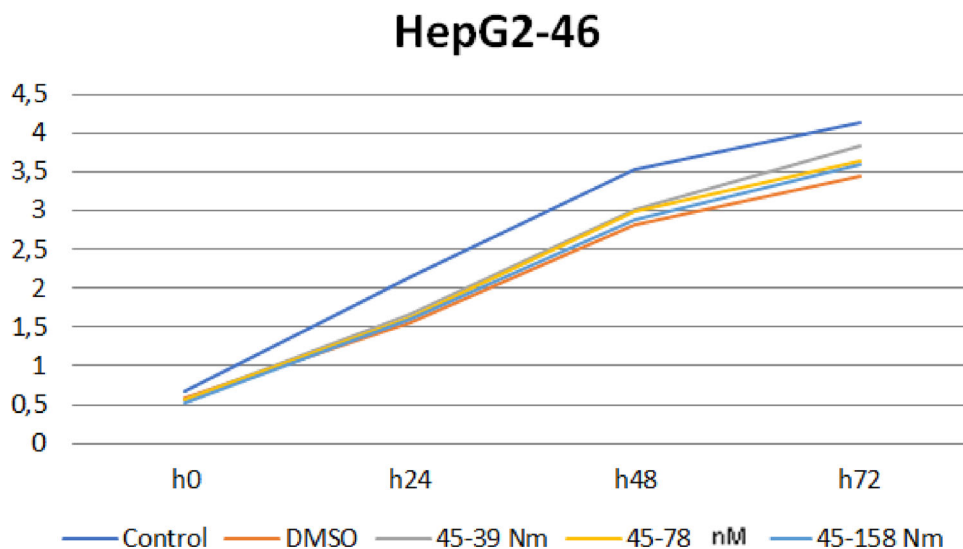


Figure 18. Cell index values of HepG2 cells treated with 39, 78, 158 nM of 46.

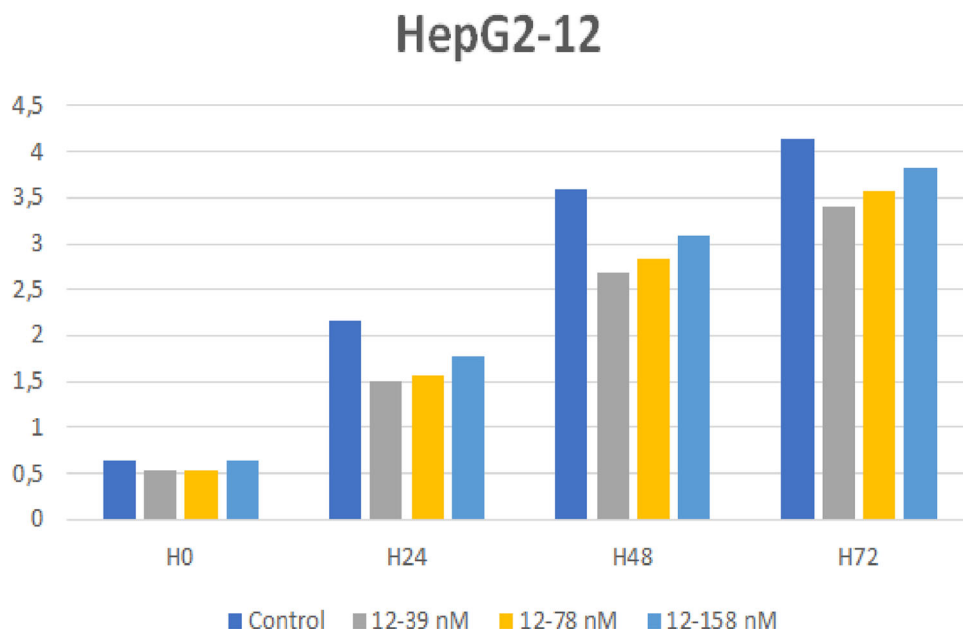


Figure 19. Determination of the concentration of 12 that is required for cell proliferation and cell viability. (A) HepG2 cells were incubated with 39, 78 and 158 nM were followed for 72 h using xCELLigence cell analysis system. UT column corresponds to untreated cells and 39, 78, 158 nM concentrations. This allows to follow in real time proliferation of the cells and to image the cells at different times. Representative images after 72 h of treatment are shown for each condition.

Also, in the binding site, positive charge interaction was found with Lys B:352. The docking score of the compound 48 was determined as $-8.48 \text{ kcal/mol}^{-1}$.

These docking results revealed that the four compounds (12, 45, 46 and 48) interacted with several common residues (Asn B:258, Thr A:179, Ala A:180, Leu B:255 and Lys B:352) when compared to the reference molecule. When the glide score values of the molecular dockings were examined, it was determined that compound 48 had the best interaction energy ($8.48 \text{ kcal mol}^{-1}$) in all the docked compounds. In addition, one of the most important findings in this study is that the docking results of the compounds with the best anticancer effect are better than the reference molecule. Figures 21 and 22 represent the docked poses of combretastatin, 12, 45, 46 and 48 compounds in the tubulin as two and three dimension, respectively.

In addition, pharmacokinetic properties such as absorption, distribution, metabolism and excretion (ADME) are important for the usability of the compounds in human therapy (Kalani et al., 2012). ADME calculations of the chalcone derivatives (12, 45, 46 and 48) were obtained using QikProp (details are provided in the Supplementary content in Table S1). In the Lipinski rules, which also consider the numbers of hydrogen bond donor-hydrogen bond acceptor atoms, molecular mass and octanol - water distribution coefficients, no deviation was observed for all these compounds (12, 45, 46 and 48) (Lipinski et al., 1997). In addition, the number of deviations from the Jorgensen rule for these compounds (12, 45, 46 and 48) was determined as 0. This result says that the compounds are more likely to be obtained orally (Duffy & Jorgensen, 2000). The compounds (12, 45, 46 and 48) have QikProp parameters within the acceptable range, except for

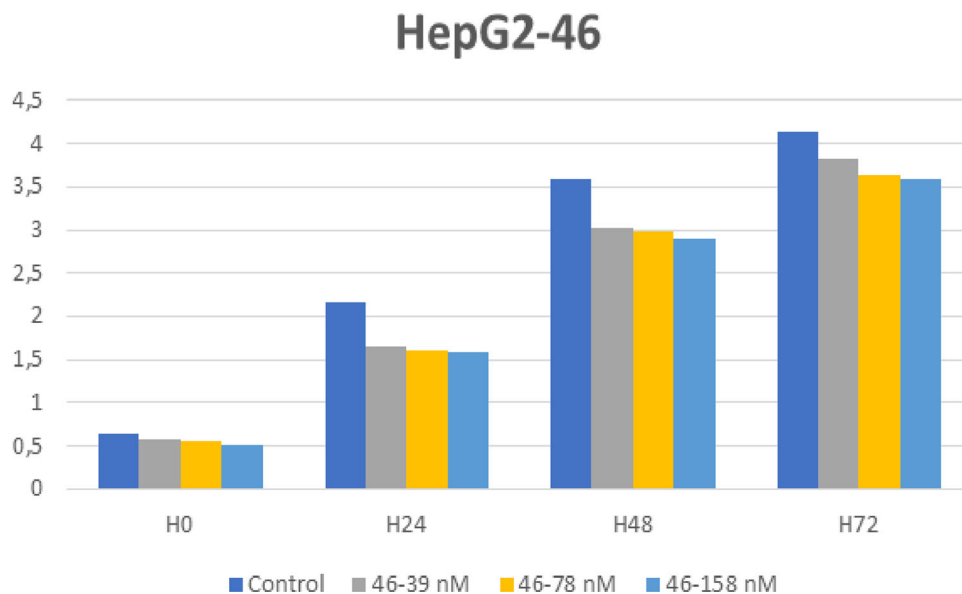


Figure 20. Determination of the concentration of **46** that is required for cell proliferation and cell viability. (A) HepG2 cells were incubated with 39, 78 and 158 nM were followed for 72 h using xCELLigence cell analysis system. UT column corresponds to untreated cells and 39,78,158 nM concentrations. This allows to follow in real time proliferation of the cells and to image the cells at different times. Representative images after 72 h of treatment are shown for each condition.

(QPlogBB, QPlogKp, and QPlogKhsa) parameters. Consequently, the estimated pharmacological properties obtained for these compounds would help design and develop more effective drug candidates in the biological system.

Conclusion

In this study, we designed and synthesized a series of novel 34 compounds. These compounds were further compared to 12 previously synthesized compounds with known biological activities as antiproliferative agents. These pharmacophore chalcones were tagged with fluoro atom(s) in B rings to further strengthen their antiproliferative activities. These compounds were synthesized by using an efficient reaction method. Their biological activities were examined in vitro against a panel of human cancer cell lines. Furthermore, the structure-activity relationship for each of the compound was determined. These compounds exerted their antiproliferative effect partially through apoptosis, the monitoring of cell viability by the xCELLigence system and also possibly by inhibiting the cell division through inhibition of microtubule formation.

Among the synthesized compounds, **12** showed the most promising anticancer activity against the majority of the cell lines. Compounds numbered with **8**, **43**, **46**, **48**, **52**, **55** and **73** were active against all of the tested cancer cell types A549, A498, HeLa, A375, and HepG2. Each of the compounds is listed with the cancer type that it was the most effective as in the following: **8**, **9**, **12**, **43**, **46**, **48-55**, **66**, **69** (0.12-0.16 μ M against A549), **8**, **12**, **48-55**, **66** and **71** (0.30-0.17 μ M against A498), **12**, **16**, **46** and **52** (0.060-0.068 μ M against HeLa), **8**, **12** and **52** (0.060-0.068 μ M against A375), and **12**, **43** and **46** (0.029-0.068 μ M against HepG2).

The preliminary SAR analysis suggested that the following structural criteria was required for the antiproliferative action of the synthesized compounds: (a) the removal of the ketone or double bond in the linker group of two phenyl ring in chalcone structures may increase antiproliferative activity depending on the substitution of A rings, methoxy or hydroxyl groups; (b) the presence of fluoro substituent at the B ring increases the antitumor potency originally displayed by lead **8** or **42**, but at least two fluoro substituents at 2, 5 positions of the B ring; (c) generally fluoro substituent at the ortho position of the B ring compounds was more potent against cell lines, 2,5-diF substituted compounds more potent against A549 and A498 cell lines. The methoxy substituted chalcone compounds without any substituents in the B ring were generally striking.

It is noteworthy that, the replacement of either the enone or ethylenic bridge of the chalcone with the rigid heterocyclic moieties resulted in ligands with superior antitumor potential. This information would pave the way towards the design and synthesis of chalcone derivatives with efficient anticancer activities. We have also tested the effect of our compounds on regular cell types such as unmodified breast cells and hepatic cells. Our results suggest that the doses that we used in our experiments were relatively safer against these cell types compared to the cancer cells.

Moreover, acridine orange staining studies of the compounds with the highest specificities and activities suggested that these compounds had their anticancer effects partly due to induction of apoptosis. Our compounds were compared to widely use chemotherapeutic MTX and they exerted similar anticancer effects while sparing the normal tissue based cell lines. Based on the in vitro data we can conclude that our reagents were relatively safer than MTX while having similar anticancer efficiencies. The compounds **12** and **46** determined to good specificity toward HepG2 cells. Therefore, these compounds were selected for xCELLigence

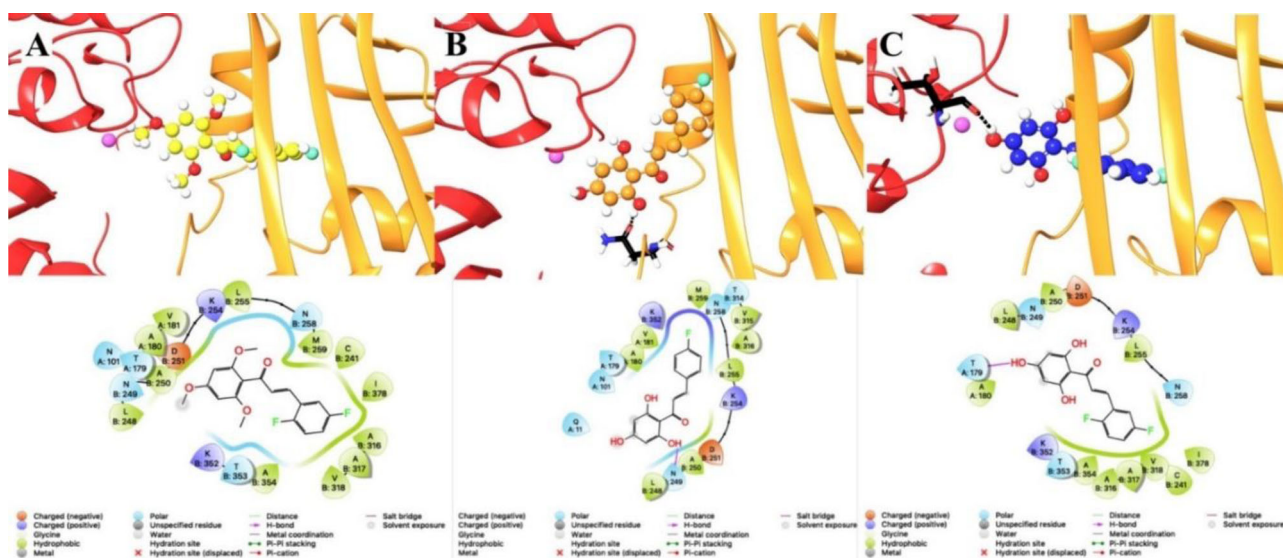


Figure 21. Molecular modeling (2D and 3D) of **12**, **45**, **46** in colchicine binding site of tubulin. Illustrated are the proposed binding mode and interaction between tubulin and selected compounds. (A) compound **12**, (B) compound **45**, (C) compound **46**. The compound **12**, **45** and **46** are represented in ball and stick model with yellow, orange and dark blue carbon atoms, respectively. In the ligands, the hydrogen atoms are white, the oxygen atoms are red, and the fluorine atoms are bright green, Mg^{2+} atom is represented as pink ball. Important amino acids in the binding pockets are shown in stick model with black carbon atoms, white hydrogen atoms, blue nitrogen atoms and red oxygen atoms, whereas tubulin is depicted in the ribbon model as red (A-chain) and yellow (B-chain).

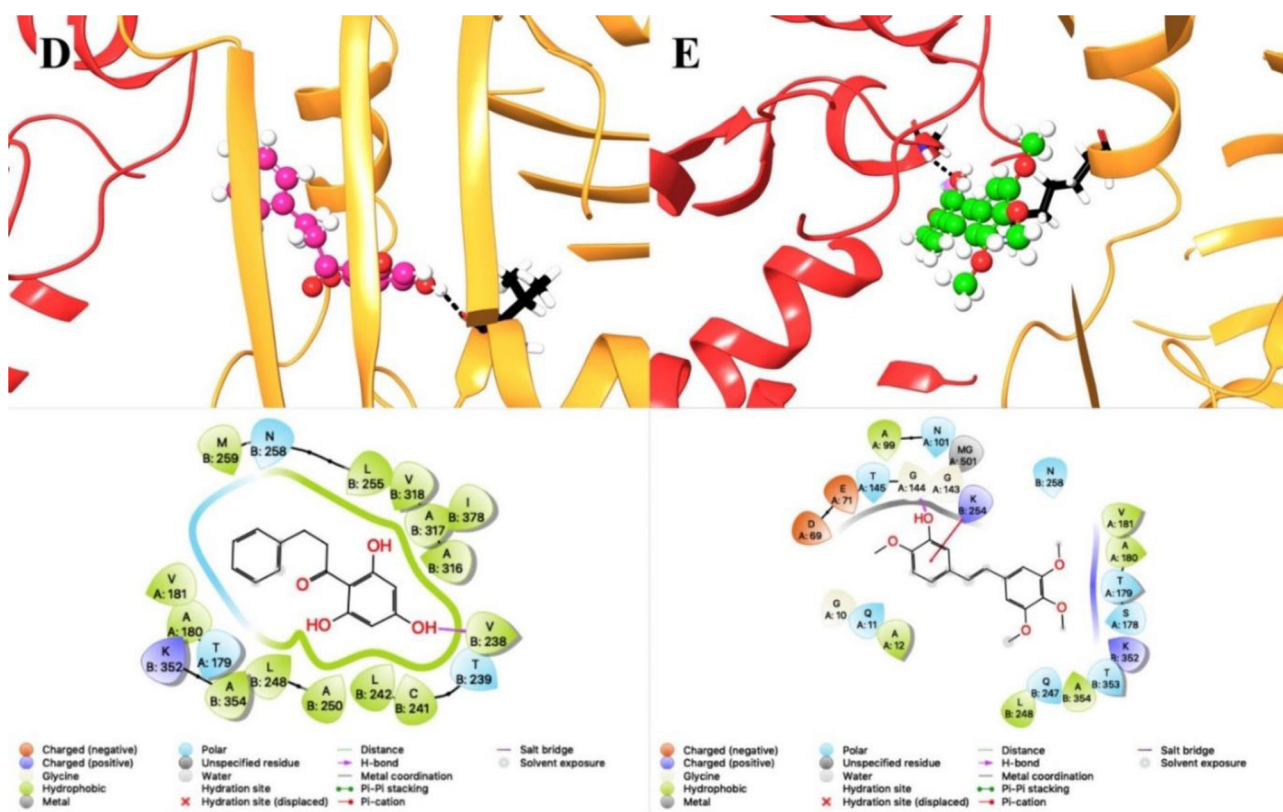


Figure 22. Molecular modeling (2D and 3D) of **48** and combretastatin-A4 in colchicine binding site of tubulin. Illustrated are the proposed binding mode and interaction between tubulin and selected compounds (D) compound **48**, (E) combretastatin-A4. The compound **48** and combretastatin-A4 are represented in ball and stick model with pink and green carbon atoms, respectively. In the ligands, the hydrogen atoms are white, the oxygen atoms are red, and the fluorine atoms are bright green, Mg^{2+} atom is represented as pink ball. Important amino acids in the binding pockets are shown in stick model with black carbon atoms, white hydrogen atoms, blue nitrogen atoms and red oxygen atoms, whereas tubulin is depicted in the ribbon model as red (A-chain) and yellow (B-chain).

assay. In order to evaluate the cytotoxicity response of BJ-5ta homo sapiens foreskin normal cell line and the liver cancer cells to the compound **12** and **46** applications, the time-dependent graph of the proliferation curves obtained from the real-time cell analyzer was plotted. The correlation is

significantly observed between the concentration of compounds (**12** and **46**) and cytotoxic response kinetics, cell index and cell viability. As a result of the xCELLigence cell analysis experiment, the difference between the mean values of the control group and the other group before

administration of the substance, the difference between the mean measurements taken at 24, 48 and 72 h after the compound **12** and **46** applications was statistically significant. For compound **12**, all concentrations except 158 mM were statistically decreased compared to control group. It has been interpreted as the development of resistance to compound **12** developed at high concentrations (158 nM).

In summary, these conclusions were in line with the results obtained from the MTT assay which supported these derivatives antiproliferative effects on different cancer cell types. In order to determine their intracellular effect, we used simulations deciphering their molecular docking on the cellular proteins. Molecular docking studies revealed that our compounds have great potential to bind tubulin dimers. Tubulins are the structural proteins that form the microtubules and microtubule formation is required for the separation of the chromosomes and other organelles at anaphase of the cell cycle. Therefore, our compounds' antiproliferative effect stems from their ability to bind tubulin and possibly by interfering the formation of the mitotic spindles consisting of microtubules.

Overall, our results suggest that these unique fluoro substituted chalcone derivatives specially **12** and **46** require further characterization to draw their pharmacokinetic effects as anticancer agents for HepG2 cancer cell lines. Also, these chalcone derivatives could provide an effective solution to improve the bioavailability and cell growth inhibitory activity against specially HepG2 cancer cell lines. We are currently working on the synthesis and mechanism of actions and *in vivo* studies of new derivatives of chalcones. These results will be published in due course.

Experimental

Chemistry

General: All reagents used were commercially available unless otherwise specified and all solvents were distilled before use. Melting points were measured with Gallenkamp melting point devices. IR Spektra: Perkin Elmer Spectrum One FT-IR spectrometer. ¹H- and ¹³C-NMR Spectra: Varian 400 and Bruker 400 spectrometers. Elemental analysis results were obtained on a Leco CHNS-932 instrument.

General procedure for preparation of compounds 8-13, 22-27 and 68-70

To a solution of related acetophenone (**1**, **20**, **21** or **67**) (1 eq.) in MeOH (2.5 mL/1 mmol of substrate). benzaldehyde derivatives (**2-7**) (1.6 eq.) and %50 KOH solution (1.5 mL/1 mmol of substrate) were added sequentially and stirred for 15 h at room temperature. After 15 h solvent was evaporated. Crude material extracted with 2 M HCl solution (2 mL/1 mmol of substrate) and DCM (2 mL/1 mmol of substrate x 3). The combined extracts were dried over Na₂SO₄. The solvent was removed in vacuo and the remaining residue purified via flash chromatography over silica gel using gradient elution with EtOAc and Hexanes to yield compounds **8-13**, **22-27** and **68-70**.

(E)-3-phenyl-1-(2,4,6-trimethoxyphenyl)prop-2-en-1-one (8)

Yellow solid; yield 98%; R_f = (EtOAc/Hexanes 30:70) = 0.27; m.p. 85-90 °C; ¹H NMR (400 MHz, CDCl₃) δ 7.53–7.51 (m, 2H), 7.38–7.34 (m, 4H), 6.96 (d, 1H, A part of AB system, J = 16.1 Hz), 6.16 (s, 2H), 3.86 (s, 3H), 3.77 (s, 6H); ¹³C NMR (100 MHz, CDCl₃) δ 194.3, 162.5, 158.9, 144.1, 135.1, 130.2, 129.1, 128.8, 128.4, 113.9, 90.7, 55.9, 55.5; IR (KBr, cm⁻¹) Vmax 2941, 1606, 1457, 1269, 1206, 1129; Anal. calcd for C₁₈H₁₈O₄: C: 72.47; H: 6.08; Found: C: 72.10; H: 6.18.

(E)-3-(2-fluorophenyl)-1-(2,4,6-trimethoxyphenyl)prop-2-en-1-one (9)

Yellow solid; yield 92%; R_f = (EtOAc/Hexanes 30:70) = 0.23; m.p. 103-106 °C; ¹H NMR (400 MHz, CDCl₃) δ 7.59–7.50 (m, 2H), 7.36–7.30 (m, 1H), 7.17–7.13 (m, 1H), 7.09-7.01 (m, 2H), 6.16 (s, 2H), 3.86 (s, 3H), 3.78 (s, 6H); ¹³C NMR (100 MHz, CDCl₃) δ 194.2, 161.1 (d, C-16, J_{CF} = 252.1 Hz), 162.6, 159.1, 136.2 (d, C-10, J_{CF} = 3.3 Hz), 131.5 (d, C-14, J_{CF} = 8.7 Hz), 131.1 (d, C-12, J_{CF} = 5.7 Hz), 128.9 (d, C-8, J_{CF} = 2.9 Hz), 124.4 (d, C-13, J_{CF} = 3.6 Hz), 123.2 (d, C-11, J_{CF} = 11.8 Hz), 116.1 (d, C-15, J_{CF} = 21.6 Hz), 111.6, 90.7, 55.9, 55.5; IR (KBr, cm⁻¹) Vmax 2941, 1607, 1458, 1269, 1228; Anal. calcd for C₁₈H₁₇FO₄: C: 68.35; H: 5.42; Found: C: 68.09; H: 5.51.

(E)-3-(3-fluorophenyl)-1-(2,4,6-trimethoxyphenyl)prop-2-en-1-one (10)

Yellow solid; yield 91%; R_f = (EtOAc/Hexanes 30:70) = 0.3; m.p. 86-90 °C; ¹H NMR (400 MHz, CDCl₃) δ 7.35–7.19 (m, 4H), 7.11–7.02 (m, 1H), 6.94 (d, 1H, A part of AB system, J = 16.0 Hz), 6.16 (s, 2H), 3.86 (s, 3H), 3.78 (s, 6H); ¹³C NMR (100 MHz, CDCl₃) δ 193.7, 162.9 (d, C-15, J_{CF} = 241.5 Hz), 162.7, 158.9, 142.2, 137.4 (d, C-11, J_{CF} = 7.5 Hz), 130.3 (d, C-13, J_{CF} = 8.4 Hz), 130.1, 124.3 (d, C-12, J_{CF} = 2.7 Hz), 116.9 (d, C-14, J_{CF} = 21.2 Hz), 114.6 (d, C-16, J_{CF} = 21.6 Hz), 111.6, 90.8, 55.9, 55.5; IR (KBr, cm⁻¹) Vmax 2942, 1652, 1607, 1457, 1228, 1157, 1129; Anal. calcd for C₁₈H₁₇FO₄: C: 68.35; H: 5.42; Found: C: 68.16; H: 5.39.

(E)-3-(4-fluorophenyl)-1-(2,4,6-trimethoxyphenyl)prop-2-en-1-one (11)

Yellow solid; yield 80%; R_f = (EtOAc/Hexanes 30:70) = 0.27; m.p. 122-123 °C; ¹H NMR (400 MHz, CDCl₃) δ 7.52–7.48 (m, 2H), 7.32 (d, 1H, B part of AB system, J = 16 Hz), 7.07–7.01 (m, 2H), 6.87 (d, 1H, A part of AB system, J = 16 Hz), 6.15 (s, 2H), 3.84 (s, 3H), 3.76 (s, 6H); ¹³C NMR (100 MHz, CDCl₃) δ 194.1, 164.0 (d, C-20, J_{CF} = 249.8 Hz), 162.7, 159.1, 142.8, 131.5, 130.4 (d, C-18, J_{CF} = 8.4 Hz), 129.0, 116.1 (d, C-19, J_{CF} = 21.7 Hz), 111.9, 90.9, 56.1, 55.7; IR (KBr, cm⁻¹) Vmax 3502, 2941, 2841, 1651, 1599; Anal. calcd for C₁₈H₁₈O₄: C: 68.35; H: 5.42; Found: C: 68.16; H: 5.38.

(E)-3-(2,5-difluorophenyl)-1-(2,4,6-trimethoxyphenyl)prop-2-en-1-one (12)

Yellow solid; yield 80%; R_f = (EtOAc/Hexanes 30:70) = 0.4; m.p. 118-120 °C; ¹H NMR (400 MHz, CDCl₃) δ 7.48 (d, 1H, B part of AB system, J = 16.0 Hz), 7.28–7.23 (m, 2H),

7.05 – 6.98 (m, 2H), 6.16 (s, 2H), 3.86 (s, 3H), 3.78 (s, 6H); ^{13}C NMR (100 MHz, CDCl_3) δ 193.5, 162.7, 158.6 (d, C-12, $J_{\text{CF}} = 244.1$ Hz), 159.1, 157.3 (d, C-15, $J_{\text{CF}} = 248.1$ Hz), 134.4, 131.9 (d, C-9, $J_{\text{CF}} = 5.0$ Hz), 124.5 (dd, C-10, $J_{\text{CF}} = 13.9, 7.5$ Hz), 117.8 (dd, C-14, $J_{\text{CF}} = 24.2, 8.8$ Hz), 117.2 (dd, C-13, $J_{\text{CF}} = 16.3, 8.6$ Hz), 114.5 (dd, C-11, $J_{\text{CF}} = 24.3, 4.0$), 111.5, 90.8, 55.9, 55.4; IR (KBr, cm^{-1}) ν_{max} 2942, 1655, 1606, 1489, 1272, 1228, 1158, 1129; Anal. calcd for $\text{C}_{18}\text{H}_{16}\text{F}_2\text{O}_4$: C: 64.67; H: 4.82; Found: C: 64.66; H: 4.81.

(E)-3-(2,5-difluoro-4-methoxyphenyl)-1-(2,4,6-trimethoxyphenyl)prop-2-en-1-one (13)

Yellow solid; yield 70%; $R_f = (\text{EtOAc}/\text{Hexanes } 30:70) = 0.33$; m.p. 176–178 °C; ^1H NMR (400 MHz, CDCl_3) δ 7.43 (d, 1H, $J = 16.0$ Hz), 7.29 – 7.24 (m, 1H), 6.86 (d, 1H, $J = 16.4$ Hz), 6.69 – 6.65 (m, 1H), 6.15 (s, 2H), 3.89 (s, 3H), 3.85 (s, 3H), 3.77 (s, 3H); ^{13}C NMR (100 MHz, CDCl_3) δ 193.8, 162.8, 159.2 (C-4/C-6), 157.9 (dd, C-16, $J_{\text{CF}} = 256.2, 2.2$ Hz), 148.9 (dd, C-13, $J_{\text{CF}} = 242.1, 2.8$ Hz), 134.9, 131.8 (dd, C-14, $J_{\text{CF}} = 5.8, 1.5$ Hz), 129.9, 114.5 (dd, C-12, $J_{\text{CF}} = 20.5, 4.9$ Hz), 111.9, 106.5 (dd, C-11, $J_{\text{CF}} = 24.4, 2.8$ Hz), 101.7 (dd, C-15, $J_{\text{CF}} = 28.4, 1.8$ Hz), 91.0 (C-1/C-3), 56.7, 56.1, 55.7; IR (KBr, cm^{-1}) ν_{max} 2941, 1604, 1516, 1457, 1227, 1128; Anal. calcd for $\text{C}_{19}\text{H}_{18}\text{F}_2\text{O}_5$: C: 62.64; H: 4.98; Found: C: 62.50; H: 4.62.

(E)-1-(2,4-dimethoxyphenyl)-3-(2-fluorophenyl)prop-2-en-1-one (22)

Light yellow solid; yield 79%; $R_f = (\text{EtOAc}/\text{Hexanes } 30:70) = 0.5$; m.p. 55–57 °C; ^1H NMR (400 MHz, CDCl_3) δ 7.81 – 7.76 (m, 1H), 7.64 – 7.57 (m, 2H), 7.34 – 7.29 (m, 2H), 7.16 – 7.05 (m, 2H), 6.55 (dd, 1H, $J = 8.4, 2.0$ Hz), 6.48 (d, 1H, $J = 2.0$ Hz), 3.89 (s, 3H), 3.85 (s, 3H); ^{13}C NMR (100 MHz, CDCl_3) δ 190.4, 164.5, 161.8 (d, C-14, $J_{\text{CF}} = 256.2$ Hz), 160.8, 134.6, 133.2, 131.4 (d, C-15, $J_{\text{CF}} = 8.6$ Hz), 129.8 (d, C-11, $J_{\text{CF}} = 6.6$ Hz), 129.6 (d, C-10, $J_{\text{CF}} = 3.1$ Hz), 124.6 (d, C-12, $J_{\text{CF}} = 3.6$ Hz), 122.2, 120.5, 116.4 (d, C-13, $J_{\text{CF}} = 21.9$ Hz), 105.5, 98.8, 55.9, 55.8; IR (KBr, cm^{-1}) ν_{max} 2942, 1657, 1607, 1457, 1327, 1259, 1212; Anal. calcd for $\text{C}_{17}\text{H}_{15}\text{FO}_3$: C: 71.32; H: 5.28; Found: C: 71.10; H: 5.31.

(E)-1-(2,4-dimethoxyphenyl)-3-(4-fluorophenyl)prop-2-en-1-one (23)

Light yellow solid; yield 54%; $R_f = (\text{EtOAc}/\text{Hexanes } 30:70) = 0.5$; m.p. 97–99 °C; ^1H NMR (400 MHz, CDCl_3) δ 7.75 (d, 1H, $J = 8.8$ Hz), 7.65 – 7.54 (m, 3H), 7.44 (d, 1H, $J = 16.0$ Hz), 7.08 – 7.04 (m, 2H), 6.55 (dd, 1H, $J = 8.4, 2.0$ Hz), 6.48 (d, 1H, $J = 2.4$ Hz), 3.88 (s, 3H), 3.84 (s, 3H); ^{13}C NMR (100 MHz, CDCl_3) δ 190.4, 164.5, 163.9 (d, C-15, $J_{\text{CF}} = 249.4$ Hz), 160.7, 140.6, 133.1, 131.9 (d, C-10, $J_{\text{CF}} = 3.4$ Hz), 130.3 (d, C-14/C-11, $J_{\text{CF}} = 8.4$ Hz), 127.2, 122.3, 116.1 (d, C-13/C-12, $J_{\text{CF}} = 21.7$ Hz), 105.5, 98.9, 56.0, 55.8; IR (KBr, cm^{-1}) ν_{max} 2941, 1655, 1599, 1508, 1418, 1327, 1213; Anal. calcd for $\text{C}_{17}\text{H}_{15}\text{FO}_3$: C: 71.32; H: 5.28; Found: C: 71.52; H: 5.54.

(E)-3-(2,5-difluorophenyl)-1-(2,4-dimethoxyphenyl)prop-2-en-1-one (24)

Light yellow solid; yield 71%; $R_f = (\text{EtOAc}/\text{Hexanes } 30:70) = 0.56$; m.p. 107–109 °C; ^1H NMR (400 MHz, CDCl_3) δ 7.77 (d, 1H, $J = 8.8$ Hz), 7.71 (d, 1H, $J = 16$ Hz), 7.58 (d, 1H, $J = 16.0$), 7.29 – 7.24 (m, 1H), 7.06 – 6.96 (m, 2H), 6.54 (dd, 1H, $J = 8.8, 2.4$ Hz), 6.47 (d, 1H, $J = 2.4$ Hz), 3.89 (s, 3H), 3.84 (s, 3H); ^{13}C NMR (100 MHz, CDCl_3) δ 189.9, 164.7, 160.9, 158.8 (dd, C-12, $J_{\text{CF}} = 239.2, 2.1$ Hz), 157.8 (dd, C-14, $J_{\text{CF}} = 248.1, 2.3$ Hz), 133.3, 132.9, 130.7, 125.1 (dd, C-10, $J_{\text{CF}} = 14.4, 7.9$ Hz), 121.9, 117.8 (dd, C-11, $J_{\text{CF}} = 23.2, 8.9$ Hz), 117.5 (dd, C-13, $J_{\text{CF}} = 24.9, 8.5$ Hz), 114.9 (dd, C-15, $J_{\text{CF}} = 24.2, 3.5$ Hz), 105.7, 98.7, 55.9, 55.8; IR (KBr, cm^{-1}) ν_{max} 2952, 1653, 1596, 1485, 1332, 1256; Anal. calcd for $\text{C}_{17}\text{H}_{14}\text{F}_2\text{O}_3$: C: 67.10; H: 4.64; Found: C: 67.06; H: 4.68.

(E)-3-(2-fluorophenyl)-1-(4-methoxyphenyl)prop-2-en-1-one (25)

Light yellow solid; yield 51%; $R_f = (\text{EtOAc}/\text{Hexanes } 30:70) = 0.5$; m.p. 108–110 °C; ^1H NMR (400 MHz, CDCl_3) δ 8.03 (d, 2H, $J = 8.8$ Hz), 7.88 (d, 1H, $J = 16.0$ Hz), 7.67 – 7.61 (m, 2H), 7.38 – 7.34 (m, 1H), 7.20 – 7.09 (m, 2H), 6.97 (d, 2H, $J = 8.8$ Hz), 3.88 (s, 3H); ^{13}C NMR (100 MHz, CDCl_3) δ 188.8, 163.8, 161.9 (d, C-14, $J_{\text{CF}} = 252.7$ Hz), 136.8, 131.8 (d, C-15, $J_{\text{CF}} = 8.8$ Hz), 131.2, 131.1, 129.9 (d, C-8, $J_{\text{CF}} = 2.9$ Hz), 124.7 (C-11/C-12), 123.4 (d, C-10, $J_{\text{CF}} = 11.5$ Hz), 116.5 (d, C-13, $J_{\text{CF}} = 22.0$ Hz), 114.1, 55.7; IR (KBr, cm^{-1}) ν_{max} 2935, 1655, 1599, 1456, 1229; Anal. calcd for $\text{C}_{16}\text{H}_{13}\text{FO}_2$: C: 74.99; H: 5.11; Found: C: 74.92; H: 5.32.

(E)-3-(4-fluorophenyl)-1-(4-methoxyphenyl)prop-2-en-1-one (26)

White solid; yield 59%; $R_f = (\text{EtOAc}/\text{Hexanes } 30:70) = 0.5$; m.p. 119–121 °C; ^1H NMR (400 MHz, CDCl_3) δ 8.01 (d, 2H, $J = 8.8$ Hz), 7.75 (d, 1H, $J = 16.0$ Hz), 7.63 – 7.59 (m, 2H), 7.46 (d, 1H, $J = 15.6$ Hz), 7.13 – 7.04 (m, 2H), 7.1 (d, 2H, $J = 8.8$ Hz), 3.87 (s, 3H); ^{13}C NMR (100 MHz, CDCl_3) δ 188.7, 164.1 (d, C-15, $J_{\text{CF}} = 250.1$ Hz), 163.6, 142.8, 131.5 (d, C-10, $J_{\text{CF}} = 5.3$ Hz), 131.2, 131.0 (C-4/C-6), 130.5 (d, C-11/C-14, $J_{\text{CF}} = 8.5$ Hz), 121.8, 116.2 (d, C-12/C-13, $J_{\text{CF}} = 21.8$ Hz), 114.1 (C-1/C-3), 55.7; IR (KBr, cm^{-1}) ν_{max} 2936, 1654, 1598, 1506, 1227; Anal. calcd for $\text{C}_{16}\text{H}_{13}\text{FO}_2$: C: 74.99; H: 5.11; Found: C: 74.84; H: 5.22.

(E)-3-(2,5-difluorophenyl)-1-(4-methoxyphenyl)prop-2-en-1-one (27)

Light yellow solid; yield 51%; $R_f = (\text{EtOAc}/\text{Hexanes } 30:70) = 0.53$; m.p. 105–107 °C; ^1H NMR (400 MHz, CDCl_3) δ 8.08 (d, 2H, $J = 8.8$ Hz), 7.82 (d, 1H, $J = 15.6$ Hz), 7.62 (d, 1H, $J = 16.0$ Hz), 7.35 – 7.31 (m, 2H), 7.13 – 7.05 (m, 1H), 6.99 (d, 2H, $J = 8.8$ Hz), 3.89 (s, 3H); ^{13}C NMR (100 MHz, CDCl_3) δ 188.3, 163.9, 158.9 (dd, C-14, $J_{\text{CF}} = 2.4, 241.7$ Hz), 157.8 (dd, C-12, $J_{\text{CF}} = 2.4, 248.6$ Hz), 135.4, 131.1, 130.9, 125.5, 124.7 (dd, C-10, $J_{\text{CF}} = 7.9, 14.1$ Hz), 118.2 (dd, C-13, $J_{\text{CF}} = 9.0, 24.2$ Hz), 117.6 (dd, C-11, $J_{\text{CF}} = 8.5, 25.0$ Hz), 115.3 (dd, C-15, $J_{\text{CF}} = 3.4, 24.3$ Hz), 114.2, 55.7; IR (KBr, cm^{-1}) ν_{max} 2929, 1659, 1598,

1489, 1338, 1247; Anal. calcd for $C_{16}H_{12}F_2O_2$: C: 70.07; H: 4.41; Found: C: 69.93; H: 4.56.

(E)-3-(2-fluorophenyl)-1-(4-hydroxyphenyl)prop-2-en-1-one (68)

Yellow solid; yield 56%; R_f = (EtOAc/Hexanes 30:70) = 0.46; m.p. 167–169 °C; 1H NMR (400 MHz, CD_3OD) δ 8.04–7.99 (m, 2H), 7.89–7.81 (m, 3H), 7.47–7.42 (m, 1H), 7.27–7.16 (m, 2H), 6.89 (d, 2H, $J=8.4$ Hz); ^{13}C NMR (100 MHz, CD_3OD) δ 189.1, 163.1, 161.8 (d, C-15, J_{CF} = 250.7 Hz), 135.5, 132.0 (d, C-17, J_{CF} = 8.8 Hz), 131.3, 129.4, 129.0, 124.7 (d, C-13, J_{CF} = 3.6 Hz), 124.0 (d, C-12, J_{CF} = 5.3 Hz), 123.1 (d, C-11, J_{CF} = 11.4 Hz), 115.8 (d, C-14, J_{CF} = 22.1 Hz), 115.4; IR (KBr, cm^{-1}) ν_{max} 3184, 2818, 1649, 1606, 1485, 1338, 1283; Anal. calcd for $C_{15}H_{11}FO_2$: C: 74.37; H: 4.58; Found: C: 74.16; H: 4.59.

(E)-3-(4-fluorophenyl)-1-(4-hydroxyphenyl)prop-2-en-1-one (69)

Yellow solid. yield 54%; R_f = (EtOAc/Hexanes 30:70) = 0.43; m.p. 176–178 °C; 1H NMR (400 MHz, CD_3OD) δ 8.03–7.99 (m, 2H), 7.79–7.70 (m, 4H), 7.18–7.14 (m, 2H), 6.89 (d, 2H, $J=8.8$ Hz), 3.83 (bs, 1H); ^{13}C NMR (100 MHz, CD_3OD) δ 189.3, 164.2 (d, C-17, J_{CF} = 248.6 Hz), 162.9, 142.5, 131.8 (d, C-11, J_{CF} = 3.1 Hz), 131.2, 130.6 (d, C-12/C-15, J_{CF} = 8.5 Hz), 129.6, 121.6, 115.7 (d, C-13/C-14, J_{CF} = 21.9 Hz), 115.3; IR (KBr, cm^{-1}) ν_{max} 3181, 2961, 1654, 1600, 1508, 1338, 1220; Anal. calcd for $C_{15}H_{11}FO_2$: C: 74.37; H: 4.58; Found: C: 74.56; H: 4.91.

(E)-3-(2,5-difluorophenyl)-1-(4-hydroxyphenyl)prop-2-en-1-one (70)

Light yellow solid. yield 83%; R_f = (EtOAc/Hexanes 30:70) = 0.66; m.p. 190–192 °C; 1H NMR (400 MHz, CD_3OD) δ 8.03 (d, 2H, $J=8.8$ Hz), 7.87–7.79 (m, 2H), 7.70–7.64 (m, 1H), 7.24–7.17 (m, 2H), 6.90 (d, 2H, $J=8.8$ Hz); ^{13}C NMR (100 MHz, CD_3OD) δ 188.7, 163.1, 159.2 (d, C-13, J_{CF} = 240.2 Hz), 157.8 (d, C-15, J_{CF} = 244.3 Hz), 134.1, 131.4 (C-4/C-6), 129.3, 129.1, 125.1 (d, C-11, J_{CF} = 4.8 Hz), 118.3 (dd, C-14, J_{CF} = 24.4, 8.0 Hz), 117.3 (dd, C-17, J_{CF} = 25.7, 8.9 Hz), 115.4 (C-1/C-3), 114.4 (dd, C-12, J_{CF} = 25.1, 2.8 Hz); IR (KBr, cm^{-1}) ν_{max} 3318, 2956, 1604, 1487, 1338, 1220; Anal. calcd for $C_{15}H_{10}F_2O_2$: C: 69.23; H: 3.87; Found: C: 68.97; H: 4.09.

General procedure for preparation of compounds 14-19, 28-33 and 71-73

To a solution of tri/di/mono-methoxy-chalcones (**8-13**, **22-27** and **68-70**) substrates in EtOH (10 mL/1 mmol of substrate) Pd/C (20%) was added. The reaction flask was purged with hydrogen gas three times before being allowed to stir under a hydrogen balloon for 16 h at room temperature. Then, the reaction mixture was filtered and concentrated in vacuo and the remaining residue purified via flash chromatography over silica gel using gradient elution with EtOAc and Hexanes to yield compounds **14-19**, **28-33** and **71-73**.

3-Phenyl-1-(2,4,6-trimethoxyphenyl)propan-1-one (14)

Colourless liquid; yield 84%; R_f = (EtOAc/Hexanes 40:60) = 0.27; 1H NMR (400 MHz, $CDCl_3$) δ 7.43–7.09 (m, 5H), 6.10 (s, 2H), 3.81 (s, 3H), 3.75 (s, 6H), 3.13–2.98 (m, 4H); ^{13}C NMR (100 MHz, $CDCl_3$) δ 204.0, 162.2, 158.4, 141.7, 128.7, 128.5, 126.1, 113.5, 90.8, 56.3, 55.7, 46.2, 29.9; IR (KBr, cm^{-1}) ν_{max} 3420, 1608, 1455, 1340, 1206, 1125; Anal. calcd for $C_{18}H_{20}O_4$: C: 71.98; H: 6.71; Found: C: 71.89; H: 6.59.

2-(3-(2-Fluorophenyl)propyl)-1,3,5-trimethoxybenzene (15)

Colourless liquid; yield 67%; R_f = (EtOAc/Hexanes 40:60) = 0.36; 1H NMR (400 MHz, $CDCl_3$) δ 7.23–7.19 (m, 1H), 7.15–7.09 (m, 1H), 7.04–6.94 (m, 2H), 6.12 (s, 2H), 3.80 (s, 3H), 3.77 (s, 6H), 2.68–2.61 (m, 4H), 1.81–1.73 (m, 2H); ^{13}C NMR (100 MHz, $CDCl_3$) δ 161.2 (d, C-15, J_{CF} = 242.6 Hz), 159.2, 158.9, 130.4 (d, C-11, J_{CF} = 5.2 Hz), 129.9 (d, C-10, J_{CF} = 15.8 Hz), 127.9 (d, C-13, J_{CF} = 3.8 Hz), 123.7 (d, C-12, J_{CF} = 3.6 Hz), 115.9 (d, C-14, J_{CF} = 22.2 Hz), 111.3, 90.5, 55.6, 55.3, 29.5, 28.7, 22.4; IR (KBr, cm^{-1}) ν_{max} 2938, 1610, 1596, 1455, 1205, 1151, 1124; Anal. calcd for $C_{18}H_{21}FO_3$: C: 71.03; H: 6.95; Found: C: 70.78; H: 7.09.

2-(3-(3-Fluorophenyl)propyl)-1,3,5-trimethoxybenzene (16)

White solid; yield 74%; R_f = (EtOAc/Hexanes 10:90) = 0.5; m.p. 40–44 °C; 1H NMR (400 MHz, $CDCl_3$) δ 7.21–7.16 (m, 1H), 6.97–6.90 (m, 1H), 6.85–6.80 (m, 2H), 6.12 (s, 2H), 3.79 (s, 3H), 3.77 (s, 6H), 2.64–2.59 (m, 4H), 1.82–1.73 (m, 2H); ^{13}C NMR (100 MHz, $CDCl_3$) δ 162.9 (d, C-14, J_{CF} = 243.0 Hz), 159.3, 158.9, 145.9, 129.4 (d, C-12, J_{CF} = 8.3 Hz), 124.1 (d, C-11, J_{CF} = 2.7 Hz), 115.2 (d, C-15, J_{CF} = 20.6 Hz), 112.2 (d, C-13, J_{CF} = 20.9 Hz), 111.2, 90.5, 55.6, 55.3, 35.5, 30.6, 22.4; IR (KBr, cm^{-1}) ν_{max} 2939, 1611, 1595, 1455, 1205, 1152, 1118; Anal. calcd for $C_{18}H_{21}FO_3$: C: 71.03; H: 6.95; Found: C: 70.89; H: 6.97.

2-(3-(4-Fluorophenyl)propyl)-1,3,5-trimethoxybenzene (17)

White solid; yield 83%; R_f = (EtOAc/Hexanes 10:90) = 0.66; m.p. 57–58 °C; 1H NMR (400 MHz, $CDCl_3$) δ 7.16–7.13 (m, 2H), 6.96–6.91 (m, 2H), 6.13 (s, 2H), 3.81 (s, 3H), 3.78 (s, 6H), 2.62–2.59 (m, 4H), 1.75 (tt, 2H, $J=15.2$, 7.6 Hz); ^{13}C NMR (100 MHz, $CDCl_3$) δ 160.1 (d, C-13, J_{CF} = 20.8 Hz), 159.4, 159.0 (C-6/C-4), 138.9, 129.8 (d, C-15/C-11, J_{CF} = 7.7 Hz), 114.8 (d, C-14/C-12, J_{CF} = 20.8 Hz), 111.5, 90.7 (C-1/C-3), 55.9, 55.5, 35.2, 31.3, 22.5; IR (KBr, cm^{-1}) ν_{max} 3445, 2937, 1609, 1597, 1508, 1455, 1204, 1150; Anal. calcd for $C_{18}H_{21}FO_3$: C: 71.03; H: 6.95; Found: C: 71.04; H: 6.85.

2-(3-(2,5-Difluorophenyl)propyl)-1,3,5-trimethoxybenzene (18)

Colourless liquid; yield 87%; R_f = (EtOAc/Hexanes 30:70) = 0.53; 1H NMR (400 MHz, $CDCl_3$) δ 6.97–6.88 (m, 2H), 6.81–6.76 (m, 1H), 6.12 (s, 2H), 3.79 (s, 3H), 3.77 (s, 6H), 2.65–2.61 (m, 4H), 1.81–1.73 (m, 2H); ^{13}C NMR (100 MHz, $CDCl_3$) δ 158.6 (d, C-18, J_{CF} = 241.0 Hz), 159.3, 158.8, 157.1 (d, C-15, J_{CF} = 250.0 Hz), 131.6 (dd, C-13, J_{CF} = 18.7, 7.5 Hz), 116.6 (dd, C-14, J_{CF} = 23.6, 5.5 Hz), 115.6 (dd, C-16, J_{CF} =

25.3, 8.8 Hz), 113.1 (dd, C-17, $J_{CF} = 24.0$, 8.6 Hz), 110.9, 90.3, 55.6, 55.3, 28.9, 28.5, 22.3; IR (KBr, cm^{-1}) ν_{max} 2939, 1611, 1596, 1496, 1457, 1205, 1153, 1121; Anal. calcd for $\text{C}_{18}\text{H}_{20}\text{F}_2\text{O}_3$: C: 67.07; H: 6.25; Found: C: 66.72; H: 6.22.

2-(3-(2,5-Difluoro-4-methoxyphenyl)propyl)-1,3,5-trimethoxybenzene (19)

White solid; yield 80%; $R_f = (\text{EtOAc}/\text{Hexanes } 30:70) = 0.83$; m.p. 80–82 °C; ^1H NMR (400 MHz, CDCl_3) δ 6.98–6.93 (m, 1H), 6.66–6.61 (m, 1H), 6.13 (s, 2H), 3.84 (s, 3H), 3.80 (s, 3H), 3.79 (s, 6H), 2.63–2.55 (m, 4H), 1.74 (tt, 2H, $J = 15.6$, 8.0 Hz); ^{13}C NMR (100 MHz, CDCl_3) δ 159.4, 159.0 (C-4/C-6), 156.8 (dd, C-15, $J_{CF} = 239.2$, 2.3 Hz), 148.6 (dd, C-12, $J_{CF} = 239.1$, 2.7 Hz), 145.9 (d, C-13, $J_{CF} = 22.6$ Hz), 121.6 (dd, C-10, $J_{CF} = 18.7$, 6.0 Hz), 116.9 (dd, C-11, $J_{CF} = 20.1$, 7.0 Hz), 111.3, 101.6 (d, C-14, $J_{CF} = 28.9$ Hz), 90.8 (C-1/C-3), 56.7, 55.8, 55.5, 29.4, 27.9, 22.3; IR (KBr, cm^{-1}) ν_{max} 2939, 1609, 1596, 1519, 1455, 1332, 1151; Anal. calcd for $\text{C}_{19}\text{H}_{22}\text{F}_2\text{O}_4$: C: 64.76; H: 6.29; Found: C: 64.65; H: 6.00.

1-(3-(2-Fluorophenyl)propyl)-2,4-dimethoxybenzene (28)

Light yellow liquid; yield 45%; $R_f = (\text{EtOAc}/\text{Hexanes } 10:90) = 0.93$; ^1H NMR (400 MHz, CDCl_3) δ 7.26–7.15 (m, 2H), 7.10–7.00 (m, 3H), 6.48 (d, 1H, $J = 2.4$ Hz), 6.45 (dd, 1H, $J = 8.0$, 2.4 Hz), 3.82 (s, 6H), 2.77 (t, 2H, $J = 8.0$ Hz), 2.65 (t, 2H, $J = 7.6$ Hz), 1.92 (tt, 2H, $J = 15.6$, 8.0 Hz); ^{13}C NMR (100 MHz, CDCl_3) δ 161.4 (d, C-14, $J_{CF} = 243.2$ Hz), 159.3, 158.6, 130.8 (d, C-11, $J_{CF} = 5.1$ Hz), 130.15, 129.7 (d, C-10, $J_{CF} = 15.7$ Hz), 127.5 (d, C-15, $J_{CF} = 8.1$ Hz), 124.0 (d, C-12, $J_{CF} = 3.4$ Hz), 123.2, 115.3 (d, C-13, $J_{CF} = 22.3$ Hz), 103.9, 98.7, 55.6, 55.5, 30.5, 29.6, 29.0; IR (KBr, cm^{-1}) ν_{max} 2936, 2861, 2071, 1613, 1587, 1505; Anal. calcd for $\text{C}_{17}\text{H}_{19}\text{FO}_2$: C: 74.43; H: 6.98; Found: C: 74.14; H: 7.24.

1-(3-(4-Fluorophenyl)propyl)-2,4-dimethoxybenzene (29)

Yellow liquid; yield 57%; $R_f = (\text{EtOAc}/\text{Hexanes } 10:90) = 0.83$; ^1H NMR (400 MHz, CDCl_3) δ 7.18–7.15 (m, 2H), 7.05–6.96 (m, 3H), 6.47–6.44 (m, 2H), 3.81 (m, 6H), 2.67–2.59 (m, 4H), 1.89 (tt, 2H, $J = 15.6$, 8.0 Hz); ^{13}C NMR (100 MHz, CDCl_3) δ 161.4 (d, C-15, $J_{CF} = 241.3$ Hz), 159.4, 158.6, 138.5 (d, C-10, $J_{CF} = 3.0$ Hz), 130.2, 129.9 (d, C-11/C-14, $J_{CF} = 7.7$ Hz), 123.2, 115.0 (d, C-13/C-12, $J_{CF} = 20.9$ Hz), 103.9, 98.7, 55.6, 55.5, 35.1, 31.9, 29.5; IR (KBr, cm^{-1}) ν_{max} 2935, 2858, 1613, 1508, 1208; Anal. calcd for $\text{C}_{17}\text{H}_{19}\text{FO}_2$: C: 74.43; H: 6.98; Found: C: 74.25; H: 6.92.

1-(3-(2,5-Difluorophenyl)propyl)-2,4-dimethoxybenzene (30)

Colorless liquid; yield 78%; $R_f = (\text{EtOAc}/\text{Hexanes } 20:80) = 0.83$; ^1H NMR (400 MHz, CDCl_3) δ 7.03 (d, 1H, $J = 8.4$ Hz), 6.98–6.89 (m, 2H), 6.86–6.80 (m, 1H), 6.46 (d, 1H, $J = 2.4$ Hz), 6.43 (dd, 1H, $J = 8.0$, 2.4 Hz), 3.80 (s, 6H), 2.68–2.59 (m, 4H), 1.88 (tt, 2H, $J = 15.6$, 8.0 Hz); ^{13}C NMR (100 MHz, CDCl_3) δ 159.4, 158.5, 158.8 (dd, C-12, $J_{CF} = 237.7$, 2.3 Hz), 157.3 (dd, C-14, $J_{CF} = 239.2$, 2.4 Hz), 131.4 (dd, C-10, $J_{CF} = 18.7$, 7.5 Hz), 130.2, 122.9, 116.8 (dd, C-11, $J_{CF} = 23.3$,

5.3 Hz), 116.7 (dd, C-13, $J_{CF} = 25.2$, 8.6 Hz), 113.6 (dd, C-15, $J_{CF} = 23.9$, 8.5 Hz), 103.9, 98.7, 55.5, 55.4, 30.1, 29.5, 28.8; IR (KBr, cm^{-1}) ν_{max} 2936, 1613, 1495, 1464, 1208; Anal. calcd for $\text{C}_{17}\text{H}_{18}\text{F}_2\text{O}_2$: C: 69.85; H: 6.21; Found: C: 69.59; H: 6.29.

1-Fluoro-2-(3-(4-methoxyphenyl)propyl)benzene (31)

Colorless liquid; yield 47%; $R_f = (\text{EtOAc}/\text{Hexanes } 20:80) = 0.93$; ^1H NMR (400 MHz, CDCl_3) δ 7.22–7.13 (m, 4H), 7.11–7.02 (m, 2H), 6.89–6.86 (m, 2H), 3.82 (s, 3H), 2.72 (t, 2H, $J = 7.6$ Hz), 2.66 (t, 2H, $J = 8$ Hz), 1.96 (tt, 2H, $J = 15.2$, 8.8 Hz); ^{13}C NMR (100 MHz, CDCl_3) δ 161.4 (d, C-14, $J_{CF} = 243.3$ Hz), 158.0, 134.4, 130.6 (d, C-11, $J_{CF} = 5.3$ Hz), 129.6 (C-4/C-6), 129.4 (d, C-10, $J_{CF} = 15.7$ Hz), 127.7 (d, C-15, $J_{CF} = 7.9$ Hz), 124.1 (d, C-12, $J_{CF} = 3.6$ Hz), 115.4 (d, C-13, $J_{CF} = 21.9$ Hz), 113.9 (C-1/C-3), 55.5, 34.9, 32.2, 28.9; IR (KBr, cm^{-1}) ν_{max} 2934, 2860, 2061, 1879, 1612, 1512; Anal. calcd for $\text{C}_{16}\text{H}_{17}\text{FO}$: C: 78.66; H: 7.01; Found: C: 78.53; H: 7.10.

3-(4-Fluorophenyl)-1-(4-methoxyphenyl)propan-1-ol (32)

Light yellow liquid; yield 44%; $R_f = (\text{EtOAc}/\text{Hexanes } 20:80) = 0.33$; ^1H NMR (400 MHz, CDCl_3) δ 7.26 (d, 2H, $J = 8.8$ Hz), 7.14–7.11 (m, 2H), 6.99–6.94 (m, 2H), 6.89 (d, 2H, $J = 8.8$ Hz), 4.62–4.58 (m, 1H), 3.80 (s, 3H), 2.73–2.57 (m, 2H), 2.14–2.10 (m, 1H), 2.03 (s, 1H, C-OH), 2.0–1.91 (m, 1H); ^{13}C NMR (100 MHz, CDCl_3) δ 161.5 (d, C-15, $J_{CF} = 242.2$ Hz), 159.3, 137.6 (d, C-10, $J_{CF} = 3.3$ Hz), 136.8, 129.9 (d, C-11/C-14, $J_{CF} = 7.6$ Hz), 127.4 (C-4/C-6), 115.2 (d, C-13/C-12, $J_{CF} = 20.8$ Hz), 114.2 (C-1/C-3), 73.6, 55.5, 40.7, 31.4; IR (KBr, cm^{-1}) ν_{max} 3387, 2933, 1709, 1610, 1509; Anal. calcd for $\text{C}_{16}\text{H}_{17}\text{FO}_2$: C: 73.83; H: 6.58; Found: C: 73.67; H: 6.71.

1,4-Difluoro-2-(3-(4-methoxyphenyl)propyl)benzene (33)

Colorless liquid; yield 73%; $R_f = (\text{EtOAc}/\text{Hexanes } 20:80) = 0.93$; ^1H NMR (400 MHz, CDCl_3) δ 7.13 (d, 2H, $J = 8.4$ Hz), 6.99–6.93 (m, 1H), 6.91–6.82 (m, 4H), 3.81 (s, 3H), 2.68–2.61 (m, 4H), 1.93 (tt, 2H, $J = 15.2$, 7.6 Hz); ^{13}C NMR (100 MHz, CDCl_3) δ 158.8 (dd, C-12, $J_{CF} = 242.3$, 2.3 Hz), 158.1, 157.3 (dd, C-14, $J_{CF} = 239.1$, 2.5 Hz), 134.1, 131.1 (dd, C-10, $J_{CF} = 18.7$, 7.7 Hz), 129.6 (C-4/C-6), 116.9 (dd, C-11, $J_{CF} = 23.3$, 5.3 Hz), 116.2 (dd, C-13, $J_{CF} = 25.4$, 8.9 Hz), 114.0 (C-1/C-3), 113.8 (dd, C-15, $J_{CF} = 24.1$, 8.7 Hz), 55.5, 34.7, 31.8, 28.8; IR (KBr, cm^{-1}) ν_{max} 2935, 2861, 1612, 1513, 1495, 1246; Anal. calcd for $\text{C}_{16}\text{H}_{16}\text{F}_2\text{O}$: C: 73.27; H: 6.15; Found: C: 73.31; H: 6.28.

4-(3-(2-Fluorophenyl)propyl)phenol (71)

Light yellow liquid; yield 50%; $R_f = (\text{EtOAc}/\text{Hexanes } 20:80) = 0.56$; ^1H NMR (400 MHz, CDCl_3) δ 7.20–7.15 (m, 2H), 7.08–6.99 (m, 4H), 6.77 (d, 2H, $J = 8.4$ Hz), 4.96 (bs, 1H), 2.68 (t, 2H, $J = 7.6$ Hz), 2.61 (t, 2H, $J = 7.6$ Hz), 1.92 (tt, 2H, $J = 15.6$, 8.0 Hz); ^{13}C NMR (100 MHz, CDCl_3) δ 161.4 (d, C-16, $J_{CF} = 243$ Hz), 153.7, 134.6, 130.8 (d, C-12, $J_{CF} = 20.8$ Hz), 129.7 (C-4/C-6), 129.3 (d, C-11, $J_{CF} = 15.8$ Hz), 127.6 (d, C-14, $J_{CF} = 8$ Hz), 124.1 (d, C-13, $J_{CF} = 3.5$ Hz), 115.4 (d, C-15, $J_{CF} = 22.1$ Hz), 115.3 (C-3/C-1), 34.8, 32.2, 28.8; IR (KBr, cm^{-1}) ν_{max}

3336, 2931, 1612, 1513, 1491, 1355, 1227; Anal. calcd for C₁₅H₁₅FO: C: 78.24; H: 6.57; Found: C: 78.13; H: 6.47.

3-(4-Fluorophenyl)-1-(4-hydroxyphenyl)propan-1-one (72)

White solid; yield 50%; R_f = (EtOAc/Hexanes 30:70) = 0.6; m.p. 133–135 °C; ¹H NMR (400 MHz, CD₃OD) δ 7.81 (d, 2H, J = 8.8 Hz), 7.20–7.15 (m, 2H), 6.94–6.89 (m, 2H), 6.81 (d, 2H, J = 8.8 Hz), 3.15 (t, 2H, J = 7.6 Hz), 2.90 (t, 2H, J = 7.2 Hz); ¹³C NMR (100 MHz, CD₃OD) δ 199.0, 162.8, 161.6 (d, C-14, J_{CF} = 241.0 Hz), 137.4 (d, C-11, J_{CF} = 3.3 Hz), 130.7 (C-4/C-6), 129.9 (d, C-16/C-12, J_{CF} = 7.6 Hz), 128.8, 115.1 (C-1/C-3), 114.8 (d, C-15/C-13, J_{CF} = 21.3 Hz), 39.6, 29.5; IR (KBr, cm⁻¹) V_{max} 3296, 2928, 1656, 1601, 1581, 1366, 1211; Anal. calcd for C₁₅H₁₃FO₂: C: 73.76; H: 5.36; Found: C: 73.58; H: 5.24.

4-(3-(2,5-Difluorophenyl)propyl)phenol (73)

White solid; yield 54%; R_f = (EtOAc/Hexanes 20:80) = 0.56; m.p. 47–49 °C; ¹H NMR (400 MHz, CDCl₃) δ 7.05 (d, 2H, J = 7.6 Hz), 6.98–6.92 (m, 1H), 6.89–6.80 (m, 2H), 6.76 (d, 2H, J = 8.4 Hz), 4.62 (bs, 1H), 2.65–2.58 (m, 4H), 1.89 (tt, 2H, J = 15.6, 8.0 Hz); ¹³C NMR (100 MHz, CDCl₃) δ 158.8 (d, C-13, J_{CF} = 232.9 Hz), 157.3 (d, C-16, J_{CF} = 238 Hz), 153.8, 134.3, 131.1 (dd, C-11, J_{CF} = 19.0, 7.7 Hz), 129.7 (C-4/C-6), 116.9 (d, C-12, J_{CF} = 23.5, 5.4 Hz), 116.2 (d, C-15, J_{CF} = 25.6, 9.0 Hz), 115.4 (C-1/C-3), 113.8 (d, C-14, J_{CF} = 23.9, 8.5 Hz), 34.7, 31.8, 28.8; IR (KBr, cm⁻¹) V_{max} 3325, 2931, 1612, 1513, 1494, 1209; Anal. calcd for C₁₅H₁₄F₂O: C: 72.57; H: 5.68; Found: C: 72.81; H: 5.89.

General procedure for preparation of compounds 42–46, 61–63

MOM protection part: To a solution of trihydroxy acetophenone (**34**) or dihydroxy acetophenone (**56**) in DCM (5 mL/1 mmol of substrate) was added DIPEA (2.9 eq.). After stirred for 0.5 h MOMCl (2.1 eq.) was added at 0 °C, under N₂ atm. Reaction mixture stirred for 3 h. Reaction stopped with saturated NH₄Cl solution (2 mL/1 mmol of substrate). The combined extracts were dried over Na₂SO₄. The solvent was removed in vacuo and the remaining residue purified via column chromatography over silica gel using gradient elution with EtOAc and Hexanes to yield compounds **35** and **57**.

Condensation part: To a solution of compounds **35** or **57** (1 eq.) in MeOH (5 mL/1 mmol of substrate) benzaldehyde derivatives (**2-7**) (1.6 eq.) and %50 KOH solution (1.5 mL/1 mmol of substrate) was added sequentially and stirred for 15 h at room temperature. After 15 h solvent was evaporated. Crude material extracted with 2 M HCl solution (2 mL/1 mmol of substrate) and EtOAc (2 mL/1 mmol of substrate x 3). The combined extracts were dried over Na₂SO₄. The solvent was removed in vacuo and the remaining residue purified via flash chromatography over silica gel using gradient elution with EtOAc and Hexanes to yield compounds **36-40** and **58-60**.

Deprotection part: To a solution of MOM-protected chalcones (**36-40** and **58-60**) (1 eq.) in EtOAc (3 mL/1 mmol

of substrate) was added 12 M HCl solution (2 eq.) drop by drop at room temperature. Reaction mixture stirred for 12 h. After 12 h reaction mixture washed with H₂O solution (2 mL/1 mmol of substrate) and extracted with EtOAc (2.5 mL/1 mmol of substrate x 3). The combined extracts were dried over Na₂SO₄. The solvent was removed in vacuo and the remaining residue purified via flash chromatography over silica gel using gradient elution with EtOAc and Hexanes to yield compounds **42-46** and **61-63**.

(E)-3-phenyl-1-(2,4,6-trihydroxyphenyl)prop-2-en-1-one (42)

Orange solid; yield 49%; R_f = (EtOAc/Hexanes 60:40) = 0.28; m.p. 193 °C; ¹H NMR (400 MHz, CD₃OD) δ 8.25–8.20 (m, 1H), 7.80–7.74 (m, 1H), 7.65–7.58 (m, 2H), 7.45–7.35 (m, 3H), 4.84 (s, 2H), 3.30 (bs, 1H); ¹³C NMR (100 MHz, CD₃OD) δ 193.3, 162.3, 161.9, 142.6, 135.7, 130.1, 128.8, 128.3, 127.3, 105.7, 104.9; IR (KBr, cm⁻¹) V_{max} 3159, 2324, 1624, 1591, 1437, 1401, 1338; Anal. calcd for C₁₅H₁₂O₄: C: 70.31; H: 4.72; Found: C: 70.29; H: 4.79.

(E)-3-(2-fluorophenyl)-1-(2,4,6-trihydroxyphenyl)prop-2-en-1-one (43)

Orange solid; yield 70%; R_f = (EtOAc/Hexanes 50:50) = 0.53; m.p. 195–197 °C; ¹H NMR (400 MHz, Acetone-d₆) δ 8.36 (d, 1H, J = 16.0 Hz), 7.89 (d, 1H, J = 15.6 Hz), 7.79–7.75 (m, 1H), 7.49–7.43 (m, 1H), 7.28–7.19 (m, 2H), 6.01 (s, 2H); ¹³C NMR (100 MHz, Acetone-d₆) δ 193.0, 165.9, 165.8, 162.3 (d, C-18, J_{CF} = 250.0 Hz), 134.5 (d, C-12, J_{CF} = 3.3 Hz), 132.7 (d, C-16, J_{CF} = 8.8 Hz), 130.9 (d, C-14, J_{CF} = 6.0 Hz), 130.1 (d, C-11, J_{CF} = 3.0 Hz), 125.7 (d, C-15, J_{CF} = 3.6 Hz), 124.3 (d, C-13, J_{CF} = 11.6 Hz), 116.9 (d, C-17, J_{CF} = 21.9 Hz), 105.7, 96.4; IR (KBr, cm⁻¹) V_{max} 3411, 1621, 1508, 1331, 1136, 1088; Anal. Calcd for C₁₅H₁₁FO₄: C: 65.69; H: 4.04; Found: C: 65.83; H: 4.04.

(E)-3-(3-fluorophenyl)-1-(2,4,6-trihydroxyphenyl)prop-2-en-1-one (44)

Orange solid; yield 39%; R_f = (EtOAc/Hexanes 60:40) = 0.5; m.p. 190 °C; ¹H NMR (400 MHz, CD₃OD) δ 8.18 (d, 1H, J = 16.0 Hz), 7.66 (d, 1H, J = 15.6 Hz), 7.42–7.38 (m, 1H), 7.34–7.30 (m, 2H), 7.14–7.06 (m, 1H), 4.85 (s, 2H), 3.31 (s, 1H); ¹³C NMR (100 MHz, CD₃OD) δ 192.5, 165.5, 164.9 (C-6/C-4), 163.3 (d, C-16, J_{CF} = 243.6 Hz), 139.9, 138.4 (d, C-12, J_{CF} = 7.6 Hz), 130.5 (d, C-14, J_{CF} = 8.3 Hz), 130.3 (d, C-13, J_{CF} = 8.3 Hz), 129.3 (C-1/C-3), 124.2, 116.3 (d, C-15, J_{CF} = 21.6 Hz), 113.9 (d, C-17, J_{CF} = 22.0 Hz), 104.8; IR (KBr, cm⁻¹) V_{max} 3203, 2917, 1626, 1585, 1448, 1344; Anal. calcd for C₁₅H₁₁FO₄: C: 65.69; H: 4.04; Found: C: 65.80; H: 3.75.

(E)-3-(4-fluorophenyl)-1-(2,4,6-trihydroxyphenyl)prop-2-en-1-one (45)

Dark yellow solid; yield 55%; R_f = (EtOAc/Hexanes 30:70) = 0.4; m.p. 161–163 °C; ¹H NMR (400 MHz, CD₃OD) δ 8.14 (d, 2H, J = 15.7 Hz), 7.71–7.64 (m, 3H), 7.17–7.12 (m, 2H), 5.85 (s, 2H), 4.89 (bs, 2H), 3.30 (bs, 1H); ¹³C NMR (100 MHz, CD₃OD) δ 192.6, 165.4, 164.9, 163.9 (d, C-17, J_{CF} = 247.8 Hz), 140.3,

132.3 (d, C-14, $J_{CF} = 3.2$ Hz), 130.2 (d, C-15/C-19, $J_{CF} = 8.4$ Hz), 127.6, 115.7 (d, C-16/C-18, $J_{CF} = 22.0$ Hz), 104.7, 94.8 (C-1/C-3); IR (KBr, cm^{-1}) ν_{max} 3294, 2931, 2481, 1599, 1509, 1353, 1219; Anal. calcd for $\text{C}_{15}\text{H}_{11}\text{FO}_4$: C: 65.69; H: 4.04; Found: C: 65.48; H: 4.35.

(E)-3-(2,5-difluorophenyl)-1-(2,4,6-trihydroxyphenyl) prop-2-en-1-one (46)

Dark orange solid; yield 40%; $R_f = (\text{EtOAc}/\text{Hexanes } 50:50) = 0.5$; m.p. 203–207 °C; ^1H NMR (400 MHz, Acetone- d_6) δ 8.32 (d, 1H, $J = 16.0$ Hz), 7.79 (d, 1H, $J = 16.0$ Hz), 7.52–7.48 (m, 1H), 7.29–7.19 (m, 2H), 6.00 (s, 2H); ^{13}C NMR (100 MHz, Acetone- d_6) δ 192.7, 166.1, 165.8, 159.7 (d, C-15, $J_{CF} = 239.5$ Hz), 158.3 (d, C-18, $J_{CF} = 246.1$ Hz), 133.1, 132.2 (d, C-12, $J_{CF} = 5.8$ Hz), 125.8 (dd, C-13, $J_{CF} = 14.3$, 7.9 Hz), 118.8 (dd, C-14, $J_{CF} = 24.6$, 9.2 Hz), 118.4 (dd, C-16, $J_{CF} = 25.1$, 8.9 Hz), 115.5 (dd, C-17, $J_{CF} = 24.7$, 3.4 Hz), 105.9, 96.1; IR (KBr, cm^{-1}) ν_{max} 3280, 1738, 1633, 1517, 1350, 1218; Anal. Calcd for $\text{C}_{15}\text{H}_{10}\text{F}_2\text{O}_4$: C: 61.65; H: 3.45; Found: C: 61.31; H: 3.76.

(E)-1-(2,4-dihydroxyphenyl)-3-(2-fluorophenyl)prop-2-en-1-one (61)

Yellow solid; yield 42%; $R_f = (\text{EtOAc}/\text{Hexanes } 30:70) = 0.5$; m.p. 160–162 °C; ^1H NMR (400 MHz, CD_3OD) δ 7.97–7.93 (m, 2H), 7.88–7.81 (m, 2H), 7.46–7.41 (m, 1H), 7.26–7.15 (m, 2H), 6.41 (dd, 1H, $J = 8.8$, 2.4 Hz), 6.29 (d, 1H, $J = 2.4$ Hz); ^{13}C NMR (100 MHz, CD_3OD) δ 191.7, 166.5, 165.6, 161.8 (d, C-15, $J_{CF} = 250.9$ Hz), 135.6, 132.4, 132.1 (d, C-18, $J_{CF} = 8.9$ Hz), 129.1, 124.7 (d, C-11, $J_{CF} = 3.5$ Hz), 122.9 (m, C-12/C-13), 115.9 (d, C-14, $J_{CF} = 22$ Hz), 113.4, 108.2, 102.7; IR (KBr, cm^{-1}) ν_{max} 3300, 1635, 1569, 1455, 1366, 1229; Anal. calcd for $\text{C}_{15}\text{H}_{11}\text{FO}_3$: C: 69.76; H: 4.29; Found: C: 69.41; H: 4.52.

(E)-1-(2,4-dihydroxyphenyl)-3-(4-fluorophenyl)prop-2-en-1-one (62)

Yellow solid; yield 76%; $R_f = (\text{EtOAc}/\text{Hexanes } 30:70) = 0.5$; m.p. 179–181 °C; ^1H NMR (400 MHz, CD_3OD) δ 7.96 (d, 1H, $J = 8.8$ Hz), 7.80–7.68 (m, 4H), 7.18–7.10 (m, 2H), 6.41 (dd, 1H, $J = 8.8$, 2.4 Hz), 6.29 (d, 1H, $J = 2.4$ Hz); ^{13}C NMR (100 MHz, CD_3OD) δ 191.9, 166.4, 165.5, 164.3 (d, C-18, $J_{CF} = 248.7$ Hz), 142.6, 132.4, 131.7 (d, C-11, $J_{CF} = 3.1$ Hz), 130.7 (d, C-12/C-15, $J_{CF} = 8.3$ Hz), 120.6, 115.7 (d, C-14/C-13, $J_{CF} = 22$ Hz), 113.5, 108.1, 102.7; IR (KBr, cm^{-1}) ν_{max} 3296, 2917, 1635, 1509, 1228, 1144; Anal. calcd for $\text{C}_{15}\text{H}_{11}\text{FO}_3$: C: 69.76; H: 4.29; Found: C: 69.72; H: 3.98.

(E)-3-(2,5-difluorophenyl)-1-(2,4-dihydroxyphenyl)prop-2-en-1-one (63)

Yellow solid; yield 56%; $R_f = (\text{EtOAc}/\text{Hexanes } 30:70) = 0.56$; m.p. 201–203 °C; ^1H NMR (400 MHz, CD_3OD) δ 7.96 (d, 1H, $J = 9.2$ Hz), 7.89–7.84 (m, 2H), 7.71–7.66 (m, 1H), 7.23–7.15 (m, 2H), 6.42 (dd, 1H, $J = 8.8$, 2.4 Hz), 6.29 (d, 1H, $J = 2.4$ Hz); ^{13}C NMR (100 MHz, CD_3OD) δ 191.4, 166.6, 165.8, 159.2 (d, C-13, $J_{CF} = 242.6$ Hz), 156.8 (d, C-15, $J_{CF} = 244.8$ Hz), 134.1, 132.5, 124.4 (dd, C-11, $J_{CF} = 13.9$, 8.6 Hz), 124.2, 118.4

(dd, C-12, $J_{CF} = 25$, 9.1 Hz), 117.3 (dd, C-18, $J_{CF} = 25.4$, 8.9 Hz), 114.4 (dd, C-14, $J_{CF} = 27.9$, 3.0 Hz), 113.4, 108.3, 102.6; IR (KBr, cm^{-1}) ν_{max} 3164, 2919, 1635, 1555, 1508, 1371, 1234; Anal. calcd for $\text{C}_{15}\text{H}_{10}\text{F}_2\text{O}_3$: C: 65.22; H: 3.65; Found: C: 65.58; H: 3.89.

General procedure for preparation of compounds 48–52, 64–66

To a solution of compounds **42–46** or **61–63** in EtOAc (10 mL/1 mmol of substrate) Pd/C (20%) was added. The reaction flask was purged with hydrogen gas three times before being allowed to stir under a hydrogen balloon for 18 h at room temperature. Then, the reaction mixture was filtered and concentrated in vacuo and the remaining residue purified via flash chromatography over silica gel using gradient elution with EtOAc and Hexanes to yield compounds **48–52** and **64–66**.

3-Phenyl-1-(2,4,6-trihydroxyphenyl)propan-1-one (48)

White solid; yield 64%; $R_f = (\text{EtOAc}/\text{Hexanes } 20:80) = 0.2$; m.p. 120 °C; ^1H NMR (400 MHz, CD_3OD) δ 7.24–7.21 (m, 2H), 7.17–7.12 (m, 2H), 7.07–7.03 (m, 1H), 5.81 (s, 2H), 4.84 (s, 2H), 3.83 (s, 1H), 3.32 (t, 2H, $J = 7.6$ Hz), 2.94 (t, 2H, $J = 8.4$ Hz); ^{13}C NMR (100 MHz, CD_3OD) δ 204.9, 164.9, 164.6, 141.9, 128.3, 128.2, 127.6, 94.6, 93.7, 31.0, 27.6; IR (KBr, cm^{-1}) ν_{max} 3295, 2917, 1629, 1602, 1514, 1452, 1294; Anal. calcd for $\text{C}_{18}\text{H}_{18}\text{O}_4$: C: 69.76; H: 5.46; Found: C: 69.65; H: 5.61.

3-(2-Fluorophenyl)-1-(2,4,6-trihydroxyphenyl)propan-1-one (49)

White solid; yield 70%; $R_f = (\text{EtOAc}/\text{Hexanes } 50:50) = 0.5$; m.p. 183–186 °C; ^1H NMR (400 MHz, Acetone- d_6) δ 11.69 (brs, 2H), 9.25 (brs, 1H), 7.37–7.34 (m, 1H), 7.23–7.20 (m, 1H), 7.12–7.04 (m, 2H), 5.97 (s, 2H), 3.43 (t, 2H, $J = 7.2$ Hz), 3.04 (t, 2H, $J = 6.8$ Hz); ^{13}C NMR (100 MHz, Acetone- d_6) δ 204.79, 165.4, 165.4, 162.1 (d, C-18, $J_{CF} = 241.6$ Hz), 131.8 (d, C-14, $J_{CF} = 4.7$ Hz), 129.5 (d, C-13, $J_{CF} = 15.5$ Hz), 128.7 (d, C-16, $J_{CF} = 8.1$ Hz), 125.1, 115.8 (d, C-17, $J_{CF} = 22.0$ Hz), 105.2, 95.9, 44.5, 24.1; IR (KBr, cm^{-1}) ν_{max} 2925, 1698, 1602, 1457, 1166; Anal. calcd for $\text{C}_{15}\text{H}_{13}\text{FO}_4$: C: 65.21; H: 4.74; Found: C: 65.13; H: 5.05.

3-(3-Fluorophenyl)-1-(2,4,6-trihydroxyphenyl)propan-1-one (50)

White solid; yield 95%; $R_f = (\text{EtOAc}/\text{Hexanes } 40:60) = 0.5$; m.p. 123 °C; ^1H NMR (400 MHz, CD_3OD) δ 7.27–7.21 (m, 1H), 7.16–7.13 (m, 1H), 7.03–6.95 (m, 1H), 6.89–6.84 (m, 1H), 5.82 (s, 2H), 4.85 (bs, 2H), 3.83 (bs, 1H), 3.32 (t, 2H, $J = 7.2$ Hz), 2.95 (t, 2H, $J = 8.0$ Hz); ^{13}C NMR (100 MHz, CD_3OD) δ 204.4, 165.0, 161.7 (d, C-16, $J_{CF} = 211.4$ Hz), 160.6, 144.9, 142.9, 129.7 (d, C-14, $J_{CF} = 7.2$ Hz), 124.1 (d, C-13, $J_{CF} = 2.7$ Hz), 114.8 (d, C-17, $J_{CF} = 21.0$ Hz), 112.3 (d, C-11, $J_{CF} = 27.0$ Hz), 104.1, 30.6, 27.6; IR (KBr, cm^{-1}) ν_{max} 3295, 2917, 1630, 1522, 1450, 1248; Anal. calcd for $\text{C}_{15}\text{H}_{13}\text{FO}_4$: C: 65.21; H: 4.74; Found: C: 65.07; H: 4.36.

3-(4-Fluorophenyl)-1-(2,4,6-trihydroxyphenyl)propan-1-one (51)

White solid; yield 60%; $R_f = (\text{EtOAc/Hexanes } 30:70) = 0.23$; m.p. 103–105 °C; $^1\text{H NMR}$ (400 MHz, CD_3OD) δ 7.23–7.19 (m, 2H), 6.97–6.93 (m, 2H), 5.81 (s, 2H), 4.83 (bs, 3H), 3.30 (t, 2H, $J = 7.6$ Hz), 2.92 (t, 2H, $J = 8$ Hz); $^{13}\text{C NMR}$ (100 MHz, CD_3OD) δ 204.6, 164.9, 164.6 (C-6/C-4), 161.5 (d, C-17, $J_{CF} = 240.0$ Hz), 137.9 (d, C-14, $J_{CF} = 3.3$ Hz), 129.8 (d, C-15/C-19, $J_{CF} = 7.6$ Hz), 114.7 (d, C-16/C-18, $J_{CF} = 21$ Hz), 104.1, 94.6 (C-1/C-3), 45.7, 30.1; IR (KBr, cm^{-1}) ν_{max} 3342, 2924, 1630, 1509, 1453, 1299, 1218; Anal. calcd for $\text{C}_{15}\text{H}_{13}\text{FO}_4$: C: 65.21; H: 4.74; Found: C: 65.12; H: 4.53.

3-(2,5-Difluorophenyl)-1-(2,4,6-trihydroxyphenyl) propan-1-one (52)

White solid; yield 65%; $R_f = (\text{EtOAc/Hexanes } 50:50) = 0.47$; m.p. 156–161 °C; $^1\text{H NMR}$ (400 MHz, Acetone- d_6) δ 11.67 (brs, 2H), 9.23 (brs, 1H), 7.22–7.07 (m, 2H), 6.99 (m, 1H), 5.94 (s, 2H), 3.43 (t, 2H, $J = 7.2$ Hz), 3.02 (t, 2H, $J = 7.2$ Hz); $^{13}\text{C NMR}$ (100 MHz, Acetone- d_6) δ 203.5, 164.5, 164.4, 158.6 (d, C-15, $J_{CF} = 240.7$ Hz), 157.2 (d, C-18, $J_{CF} = 239.9$ Hz), 130.7 (dd, C-13, $J_{CF} = 18.2, 7.8$ Hz), 116.9 (dd, C-14, $J_{CF} = 24.1, 5.1$ Hz), 116.1 (dd, C-17, $J_{CF} = 25.3, 8.9$ Hz), 113.8 (dd, C-16, $J_{CF} = 24.2, 8.6$ Hz), 104.4, 94.9, 43.3, 23.7; IR (KBr, cm^{-1}) ν_{max} 3139, 1625, 1496, 1396, 1141; Anal. calcd for $\text{C}_{15}\text{H}_{12}\text{F}_2\text{O}_4$: C: 61.23; H: 4.11; Found: C: 61.47; H: 4.39.

4-(3-(2-Fluorophenyl)propyl)benzene-1,3-diol (64)

White solid; yield 69%; $R_f = (\text{EtOAc/Hexanes } 30:70) = 0.33$; m.p. 91–93 °C; $^1\text{H NMR}$ (400 MHz, CDCl_3) δ 7.26 (s, 1H), 7.21–7.13 (m, 2H), 7.07–6.95 (m, 2H), 6.35 (dd, 1H, $J = 8.0, 4.0$ Hz), 6.31 (d, 1H, $J = 2.4$ Hz), 4.81 (bs, 2H), 2.69 (t, 2H, $J = 7.6$ Hz), 2.60 (t, 2H, $J = 7.6$ Hz), 1.9 (tt, 2H, $J = 12.8, 7.6$ Hz); $^{13}\text{C NMR}$ (100 MHz, CDCl_3) δ 161.4 (d, C-18, $J_{CF} = 243.4$ Hz), 154.8, 154.5, 130.9, 130.8 (d, C-14, $J_{CF} = 5.1$ Hz), 129.3 (d, C-13, $J_{CF} = 16$ Hz), 127.7 (d, C-16, $J_{CF} = 8$ Hz), 124.1 (d, C-16, $J_{CF} = 3.4$ Hz), 120.6, 115.4 (d, C-17, $J_{CF} = 22.2$ Hz), 107.9, 103.1, 30.4, 29.1, 28.9; IR (KBr, cm^{-1}) ν_{max} 3349, 2930, 2862, 1618, 1491, 1455, 1227; Anal. calcd for $\text{C}_{15}\text{H}_{15}\text{FO}_2$: C: 73.15; H: 6.14; Found: C: 73.47; H: 6.02.

1-(2,4-Dihydroxyphenyl)-3-(4-fluorophenyl)propan-1-one (65)

White solid; yield 60%; $R_f = (\text{EtOAc/Hexanes } 40:60) = 0.66$; m.p. 125–127 °C; $^1\text{H NMR}$ (400 MHz, CDCl_3) δ 12.72 (s, 1H), 7.62 (d, 1H, $J = 8.0$ Hz), 7.21–7.17 (m, 2H), 7.0–6.96 (m, 2H), 6.36–6.34 (m, 2H), 5.62 (s, 1H), 3.21 (t, 2H, $J = 9.2$ Hz), 3.02 (t, 2H, $J = 7.6$ Hz); $^{13}\text{C NMR}$ (100 MHz, CDCl_3) δ 203.6, 164.0 (d, C-15, $J_{CF} = 273.4$ Hz), 162.9, 160.5, 136.6 (d, C-12, $J_{CF} = 3.3$ Hz), 132.4, 130.0 (d, C-17/C-13, $J_{CF} = 7.6$ Hz), 115.6 (d, C-16/C-14, $J_{CF} = 20.9$ Hz), 114.1, 107.9, 103.9, 39.9, 29.7; IR (KBr, cm^{-1}) ν_{max} 3337, 2923, 1631, 1509, 1445, 1373, 1221; Anal. calcd for $\text{C}_{15}\text{H}_{13}\text{FO}_3$: C: 69.22; H: 5.03; Found: C: 69.16; H: 5.24.

4-(3-(2,5-Difluorophenyl)propyl)benzene-1,3-diol (66)

White solid; yield 60%; $R_f = (\text{EtOAc/Hexanes } 30:70) = 0.43$; m.p. 119–121 °C; $^1\text{H NMR}$ (400 MHz, CD_3OD) δ 7.02–6.95 (m, 2H), 6.91–6.86 (m, 1H), 6.82 (d, 1H, $J = 8.0$ Hz), 6.26 (d, 1H, $J = 2.0$ Hz), 6.20 (dd, 1H, $J = 8.0, 2.4$ Hz), 4.88 (s, 1H), 3.30 (s, 1H), 2.62 (t, 2H, $J = 7.6$ Hz), 2.53 (t, 2H, $J = 7.6$ Hz), 1.82 (tt, 2H, $J = 15.6, 8.0$ Hz); $^{13}\text{C NMR}$ (100 MHz, CD_3OD) δ 158.9 (dd, C-14, $J_{CF} = 2.1, 238.9$ Hz), 157.3 (dd, C-17, $J_{CF} = 2.3, 240.1$ Hz), 156.2, 155.9, 131.6 (dd, C-12, $J_{CF} = 7.5, 18.6$ Hz), 130.2, 119.5, 116.6 (dd, C-13, $J_{CF} = 5.4, 24.9$ Hz), 115.8 (dd, C-16, $J_{CF} = 8.9, 25.6$ Hz), 113.3 (dd, C-15, $J_{CF} = 8.6, 24.2$ Hz), 106.2, 102.3, 30.3, 29.3, 28.4; IR (KBr, cm^{-1}) ν_{max} 3400, 2931, 1620, 1525, 1489, 1305, 1236; Anal. calcd for $\text{C}_{15}\text{H}_{14}\text{F}_2\text{O}_2$: C: 68.17; H: 5.34; Found: C: 67.90; H: 5.59.

Biological part**Cell culture studies**

Cytotoxicity assays against cancer cells: In this study, five different cancer cell lines were used [A549 Cell Line (Human Lung Adenocarcinoma Epithelial Cells), A498 Cell Line (Human Renal Cancer Cells), HeLa Cell Line (Human Cervical Cancer cells), A375 Cell Line (Human Skin. Malignant Melanoma Cells), HepG2 Cell Line (Human Hepatocellular Carcinoma Cells)] to investigate the anti-proliferative effects of the synthesized compounds. Other than these cancer cell lines, HEK 293 was used as the untransformed tissue originated cell line control to determine the non-toxic concentrations of the compounds on relatively healthy cells. All cell lines were obtained from the cell culture collections of Mustafa Kemal University. Cell incubations were done at 37 °C in 5% (v/v) CO_2 .

MTT cell viability assay

The cytotoxic activity of the compounds was determined by using MTT assay (McGahon et al., 1995; Mosmann, 1983). The compounds were dissolved in dimethyl sulfoxide (DMSO) and then diluted to the appropriate concentrations in Dulbecco's modified Eagle's medium (DMEM). Concentration of DMSO was less than 1% in the culture medium. Subsequently, the cells were seeded at 104 cells/well in DMEM, supplemented with 10% fetal bovine serum (FBS), 100 unit/mL penicillin-G, 100 $\mu\text{g/mL}$ streptomycin in each well of 96-well microculture plates. The cells were cultured at 37 °C for 24, 48, 72 and 96 h in an incubator containing 5% CO_2 .

After incubation, cells were treated with test compounds of appropriate concentrations for 24, 48, 72 and 96 h. After incubation period, 10 μL MTT (3-(4,5-dimethylthiazol-2-yl)-2,5-diphenyl tetrazolium bromide) (5 mg/mL) was added to each well and the plates were further incubated for 4 h. Then the medium of each well was carefully removed, formazan crystals were dissolved in 100 μL of DMSO. Absorbance was determined at 570 nm for each well using microplate reader (Bioteck) (Sabina et al., 2017).

The cell viability was expressed as percentage of the viable cells in each sample with respect to the control wells.

Three independent experiments in triplicates were done for the determination of the growth inhibition of each compound. The IC50 values were calculated from concentration-response curves using the SPSS (SPSS, Inc. Chicago) Software.

Determination of the apoptotic indexes by acridine orange staining

Acridine orange is a dye that enters the nucleic acid (DNA or RNA) structure in cells or can be attached to nucleic acids. This binding is an event that occurs as a result of electrostatic interactions of the acridine molecule between nucleic acid base pairs. Acridine orange allows cells to be examined by fluorescence microscopy due to their metachromatic properties. With this staining method, analysis of cellular physiology and cell cycle status can be performed (Mirzaei et al., 2020). The Acridine Orange dying method was performed according to the method described by Mossman (Kalani et al., 2012). For this purpose, after preparing the cell suspension to be 1×10^6 cells/mL sterile coverslips were placed in culture dishes. The new synthesized chemical compounds (at different concentrations) were added to the cell cultures at the determined concentrations and the cell cultures were incubated at 37 °C. At the end of the incubation, the cells were washed 3 times for 2 min with PBS solution. After the last wash, 1 mL of p ethanol was added to the culture dishes and kept at room temperature for 5 min. After a series of washes, the cells soaked in PBS for 2 min were treated with acridine orange diluted with PBS. Then a mixture of 200 μ L of acridine orange (100 μ g/mL) and ethidium bromide (100 μ g/mL) was added to the cells and incubated at room temperature for 5 min.

At the end of the staining process, the cell preparations were examined under an immuno-fluorescent microscope (Olympus) and evaluated. In the microscopic examination, live cells (green stained chromatin), apoptotic cells (condensate and fragmented green stained chromatin), dead cells with normal nuclei (condensed and fragmented orange stained chromatin) were counted in the preparade. Subsequently, the apoptotic index calculation was made according to the formula below.

Apoptotic index = (Number of Apoptotic Cells plus Number of Apoptotic Core Dead Cells)/Number of Live Cells plus Number of Apoptotic Cells Number of Normal Cells with Dead Nucleus plus Number of Apoptotic Nuclei) \times 100.

xCELLigence cytotoxicity studies

In order to evaluate the cytotoxicity response of the liver cancer cells to the 12 and 46 applications, the time-dependent graph of the proliferation curves obtained from the real-time cell analyser was plotted. The data obtained were digitized in terms of cell index by the software of the device. After the whole experimental procedure was prepared in the system, 100 μ L of doped medium was added to each well of the e-plates and the plates were placed in the system in the incubator. In this way, the experiment was started and blank reading was taken. Then the cell suspension containing 90 μ L of (2×10^4 HepG2 and BJ-5ta 5×10^3) cell was added to the

wells. The final volume of all wells was 190 μ L. Plates were re-placed in the incubator and the cell proliferation curve was monitored for 24 h. Different concentrations (39 nM, 78 nM and 158 nM) of 12 and 46 (200 μ L) were then added to the cells, 0.01% DMSO was used as a vehicle group and CI was measured automatically once per hour until the end of the experiment.

Molecular docking

Molecular docking studies of the synthesized chalcone derivatives were performed using the Glide XP docking protocol. Crystal structure of β -tubulin (PDB ID: 1SA0) (Mirzaei et al., 2020; Sabina et al., 2017) was prepared using Protein Preparation Wizard of Maestro. The unwanted water molecules were removed from the protein and hydrogen atoms were added. Further, the protein was optimized and minimized. The receptor-binding site was defined as a Glide enclosing box in the centroid of the co-crystallized colchicine molecule. The structures of chalcone derivatives were built in the Maestro program and prepared for docking with LigPrep tool. The process was made at neutral pH and under OPLS 2005 force field (Halgren et al., 2004). The compounds were docked into the β -tubulin structure using Glide XP (Halgren et al., 2004; Schrödinger, LLC, 2017). The best docked poses with lowest Glide score values were documented for each compound.

Prediction of ADME properties

The QikProp program of Schrödinger Maestro 9.2 (Schrödinger, LLC, 2017) was used to obtain the ADME properties of the chalcone derivatives. The program uses the Jorgensen (Duffy & Jorgensen, 2000; Jorgensen & Duffy, 2000; 2002) method to calculate pharmacokinetic properties and some identifiers. In addition, QikProp offers a range of values to compare certain molecular properties with 95% of known drugs.

Disclosure statement

No potential conflict of interest was reported by the author(s).

Funding

Scientific and Technological Research Council of Turkey 10.13039/501100004410We thank the Scientific and Technological Research Council of Turkey (TUBITAK Grant Number: 114Z554).

ORCID

Oztekin Algul  <http://orcid.org/0000-0001-5685-7511>

References

Abbot, V., Sharma, P., Dhiman, S., Noolvi, M. N., Patel, H. M., & Bhardwaj, V. (2017). Small hybrid heteroaromatics: Resourceful biological tools

- in cancer research. *RSC Advances*, 7(45), 28313–28349. <https://doi.org/10.1039/C6RA24662A>
- Banu, S., Bollu, R., Bantu, R., Nagarapu, L., Polepalli, S., Jain, N., Vangala, R., & Manga, V. (2017). Design, synthesis and docking studies of novel 1,2-dihydro-4-hydroxy-2-oxoquinoline-3-carboxamide derivatives as a potential anti-proliferative agents. *European Journal of Medicinal Chemistry*, 125, 400–410. <https://doi.org/10.1016/j.ejmech.2016.09.062>
- Bégué, J. P., & Bonnet-Delpon, D. (2008). *Bioorganic and Medicinal Chemistry of Fluorine*. John Wiley & Sons, Inc.
- Burmaoglu, S., Anil, D. A., Gobek, A., Gulbol Duran, G., Ersan, R. H., Duran, N., & Algul, O. (2016). Synthesis and anti-proliferative activity of fluoro-substituted chalcones. *Bioorganic & Medicinal Chemistry Letters*, 26(13), 3172–3176. <https://doi.org/10.1016/j.bmcl.2016.04.096>
- Choudhury, D., Xavier, P. L., Chaudhari, K., John, R., Dasgupta, A. K., Pradeep, T., & Chakrabarti, G. (2013). Unprecedented inhibition of tubulin polymerization directed by gold nanoparticles inducing cell cycle arrest and apoptosis. *Nanoscale*, 5(10), 4476–4489. <https://doi.org/10.1039/c3nr33891f>
- Duffy, E. M., & Jorgensen, W. L. (2000). Prediction of Properties from Simulations: Free Energies of Solvation in Hexadecane, Octanol, and Water. *Journal of the American Chemical Society*, 122(12), 2878–2888.
- Halgren, T. A., Murphy, R. B., Friesner, R. A., Beard, H. S., Frye, L. L., Pollard, W. T., & Banks, J. L. (2004). Glide: A new approach for rapid, accurate docking and scoring. 2. Enrichment factors in database screening. *Journal of Medicinal Chemistry*, 47(7), 1750–1759. [Database] <https://doi.org/10.1021/jm030644s>
- Huang, X., Huang, R., Li, L., Gou, S., & Wang, H. (2017). Synthesis and biological evaluation of novel chalcone derivatives as a new class of microtubule destabilizing agents. *European Journal of Medicinal Chemistry*, 132, 11–25. <https://doi.org/10.1016/j.ejmech.2017.03.031>
- Isanbor, C., & O'Hagan, D. (2006). Fluorine in medicinal chemistry: A review of anti-cancer agents. *Journal of Fluorine Chemistry*, 127(3), 303–319. <https://doi.org/10.1016/j.jfluchem.2006.01.011>
- Jorgensen, W. L., & Duffy, E. M. (2000). Prediction of drug solubility from Monte Carlo simulations. *Bioorganic & Medicinal Chemistry Letters*, 10(11), 1155–1158. [https://doi.org/10.1016/s0960-894x\(00\)00172-4](https://doi.org/10.1016/s0960-894x(00)00172-4)
- Jorgensen, W. L., & Duffy, E. M. (2002). Prediction of drug solubility from structure. *Advanced Drug Delivery Reviews*, 54(3), 355–366. [https://doi.org/10.1016/s0169-409x\(02\)00008-x](https://doi.org/10.1016/s0169-409x(02)00008-x)
- Kalani, K., Yadav, D. K., Khan, F., Srivastava, S. K., & Suri, N. (2012). Pharmacophore, QSAR, and ADME based semisynthesis and in vitro evaluation of ursolic acid analogs for anticancer activity. *J Mol Model*, 18(7), 3389–3413. <https://doi.org/10.1007/s00894-011-1327-6>
- Kamal, A., Dastagiri, D., Ramaiah, M. J., Reddy, J. S., Bharathi, E. V., Srinivas, C., Pushpavalli, S. N. C. V. L., Pal, D., & Pal-Bhadra, M. (2010). Synthesis of imidazothiazole-chalcone derivatives as anticancer and apoptosis inducing agents. *Chemmedchem*, 5(11), 1937–1947. <https://doi.org/10.1002/cmdc.201000346>
- Karthikeyan, C., Narayana Moorthy, N. S. H., Ramasamy, S., Vanam, U., Manivannan, E., Karunakaran, D., & Trivedi, P. (2014). Advances in Chalcones with Anticancer Activities. *Recent Patents on anti-Cancer Drug Discovery*, 10(1), 97–115. <https://doi.org/10.2174/1574892809666140819153902>
- Lipinski, C. A., Lombardo, F., Dominy, B. W., & Feeney, P. J. (1997). Experimental and computational approaches to estimate solubility and permeability in drug discovery and development settings. *Advanced Drug Delivery Reviews*, 23(1-3), 3–25. [https://doi.org/10.1016/S0169-409X\(96\)00423-1](https://doi.org/10.1016/S0169-409X(96)00423-1)
- Matos, M. J., Vazquez-Rodriguez, S., Uriarte, E., & Santana, L. (2015). Potential pharmacological uses of chalcones: A patent review (from June 2011 – 2014). *Expert Opinion on Therapeutic Patents*, 25(3), 351–366. <https://doi.org/10.1517/13543776.2014.995627>
- McGahon, A. J., Martin, S. J., Bissonnette, R. P., Mahboubi, A., Shi, Y., Mogil, R. J., Nishioka, W. K., & Green, D. R. (1995). The end of the (cell) line: Methods for the study of apoptosis in vitro. *Methods in Cell Biology*, 46, 153–185. [https://doi.org/10.1016/s0091-679x\(08\)61929-9](https://doi.org/10.1016/s0091-679x(08)61929-9)
- Menea, F., Menea, B., & Sharts, O. N. (2013). Importance of fluorine and fluorocarbons in medicinal chemistry and oncology. *J. Mol. Pharm. Org. Process Res*, 1, 1–6. <https://doi.org/10.4172/2329-9053.1000104>
- Mirzaei, S., Hadizadeh, F., Eivsand, F., Mosaffa, F., & Ghodsi, R. (2020). Synthesis, structure-activity relationship and molecular docking studies of novel quinoline-chalcone hybrids as potential anticancer agents and tubulin inhibitors. *Journal of Molecular Structure*, 1202, 127310. <https://doi.org/10.1016/j.molstruc.2019.127310>
- Mosmann, T. (1983). Rapid colorimetric assay for cellular growth and survival: Application to proliferation and cytotoxicity assays. *Journal of Immunological Methods*, 65(1-2), 55–63.
- Qiu, H. Y., Wang, F., Wang, X., Sun, W. X., Qi, J. L., Pang, Y. J., Yang, R. W., Lu, G. H., Wang, X. M., & Yang, Y. H. (2017). Design, Synthesis, and Biological Evaluation of Chalcone-Containing Shikonin Derivatives as Inhibitors of Tubulin Polymerization. *ChemMedChem*, 12(5), 399–406. <https://doi.org/10.1002/cmdc.201700001>
- Sabina, X. J., Karthikeyan, J., Velmurugan, G., Tamizh, M. M., & Shetty, A. N. (2017). Design and in vitro biological evaluation of substituted chalcones synthesized from nitrogen mustards as potent microtubule targeted anticancer agents. *New Journal of Chemistry*, 41(10), 4096–4109. <https://doi.org/10.1039/C7NJ00265C>
- Schrödinger, LLC. (2017). *Schrödinger Release 2017-2: Maestro*, Schrödinger, LLC.
- Schrödinger, LLC. (2017). *Schrödinger Release 2017-2: QikProp*, Schrödinger, LLC.
- Singh, P., Anand, A., & Kumar, V. (2014). Recent developments in biological activities of chalcones: a mini review. *European Journal of Medicinal Chemistry*, 85, 758–777. <https://doi.org/10.1016/j.ejmech.2014.08.033>
- Wang, G., Liu, W., Gong, Z., Huang, Y., Li, Y., & Peng, Z. (2020). Design, synthesis, biological evaluation and molecular docking studies of new chalcone derivatives containing diaryl ether moiety as potential anti-cancer agents and tubulin polymerization inhibitors. *Bioorganic Chemistry*, 95, 103565 <https://doi.org/10.1016/j.bioorg.2019.103565>